Preprint typeset in JHEP style - HYPER VERSION
OU-HEP-130801, KIAS-P13049

Mixed axion/neutralino dark matter in the SUSY DFSZ axion model

Kyu Jung Bae[a], **Howard Baer**[a] **and Eung Jin Chun**[b]

[a] *Dept. of Physics and Astronomy, University of Oklahoma, Norman, OK 73019, USA*
[b] *Korea Institute for Advanced Study, Seoul 130-722, Korea*
E-mail: bae@nhn.ou.edu, baer@nhn.ou.edu, ejchun@kias.re.kr

Abstract: We examine mixed axion/neutralino cold dark matter production in the SUSY DFSZ axion model where an axion superfield couples to Higgs superfields. We calculate a wide array of axino and saxion decay modes along with their decay temperatures, and thermal and non-thermal production rates. For a SUSY benchmark model with a standard underabundance (SUA) of Higgsino-like dark matter (DM), we find for the PQ scale $f_a \lesssim 10^{12}$ GeV that the DM abundance is mainly comprised of axions as the saxion/axino decay occurs before the standard neutralino freeze-out and thus its abundance remains suppressed. For $10^{12} \lesssim f_a \lesssim 10^{14}$ GeV, the saxion/axino decays occur after neutralino freeze-out so that the neutralino abundance is enhanced by the production via decay and subsequent re-annihilation. For $f_a \gtrsim 10^{14}$ GeV, both neutralino dark matter and dark radiation are typically overproduced. For judicious parameter choices, these can be suppressed and the combined neutralino/axion abundance brought into accord with measured values. A SUSY benchmark model with a standard overabundance (SOA) of bino DM is also examined and typically remains excluded due at least to too great a neutralino DM abundance for $f_a \lesssim 10^{15}$ GeV. For $f_a \gtrsim 10^{15}$ GeV and lower saxion masses, large entropy production from saxion decay can dilute all relics and the SOA model can be allowed by all constraints.

Keywords: DFSZ.

1. Introduction

The recent discovery of a Higgs boson at the LHC seemingly completes the discovery program for all matter states predicted by the Standard Model (SM). And yet the SM in the present form is beset by two problems – the strong CP problem in the QCD sector and the instability of scalar fields under quantum corrections (the infamous quadratic divergences) in the electroweak sector. The first of these can be solved by introducing a Peccei-Quinn (PQ) symmetry [1] and a concomitant *axion* field a [2]. The PQ symmetry is broken at a scale f_a typically taken to be in the range $f_a \sim 10^9 - 10^{12}$ GeV [3, 4]. By introducing the new PQ scale f_a into the model, one might then expect the new scalar mass m_h to blow up to at least the PQ scale. The Higgs mass can be stabilized by introducing softly broken supersymmetry (SUSY), where the soft SUSY breaking (SSB) terms are expected to be of order the gravitino mass $m_{3/2}$ in gravity-mediated SUSY breaking models [5]. In this case, the axion is but one element of an axion chiral superfield A which necessarily also includes an R-parity-even spin-zero saxion s and an R-parity-odd spin-1/2 axino $\tilde{a}$. In gravity-mediation, the saxion is expected to obtain a SSB mass $m_s \sim m_{3/2}$. The axino is also expected to obtain a mass $m_{\tilde{a}} \sim m_{3/2}$ unless special circumstances arise [6, 7, 8].[1] For R-parity conserving SUSY models – as motivated by the need for proton stability – the dark matter is then expected to consist of both an axion and the lightest SUSY particle (LSP), *i.e. two dark matter particles*. The LSP in gravity-mediation, which is assumed here, is typically the lightest neutralino $\widetilde{Z}_1$, a WIMP candidate. Thus, in this class of models, it is conceivable that both a WIMP and an axion might be detected in dark matter search experiments.

To assess dark matter detection prospects, one must calculate the ultimate abundance of both axions and WIMPs. The calculation is considerably more involved than in the axion-only [9, 10] or the WIMP-only case [11]. In the PQ augmented Minimal Supersymmetric Standard Model (PQMSSM), one may produce WIMPs thermally, but also non-thermally via production and subsequent decay of both axinos and saxions. In addition, late decay of saxions and axinos into SM particles after WIMP freeze-out but before onset of Big-Bang Nucleosynthesis (BBN) can inject entropy and thus dilute all relics present at the time of decay. Thus, the ultimate axion/WIMP abundance also depends on the production and decay of both saxions and axinos in the early universe.

The axion-axino-saxion kinetic terms and self-couplings (in four component notation) are of the form

$$\mathcal{L} = \left(1 + \frac{\sqrt{2}\xi}{v_{PQ}} s\right) \left[\frac{1}{2}\partial^\mu a \partial_\mu a + \frac{1}{2}\partial^\mu s \partial_\mu s + \frac{i}{2}\bar{\tilde{a}}\partial\!\!\!/\tilde{a}\right] \tag{1.1}$$

where $\xi = \sum_i q_i^3 v_i^2 / v_{PQ}^2$. Here q_i and v_i denote PQ charges and vacuum expectation values of PQ fields S_i, and the PQ scale $v_{PQ} = f_a/\sqrt{2}$ is given by $v_{PQ} = \sqrt{\sum_i q_i^2 v_i^2}$. In the above interaction, ξ is typically ~ 1, but in some cases can be as small as ~ 0 [8].

The axino/saxion production/decay rates are model-dependent. In the SUSY KSVZ case, where heavy quark superfields Q and Q^c are introduced to implement the PQ sym-

[1] Such a heavy axino cannot be a dark matter candidate as it is overproduced by thermal scattering as will be discussed later.

metry, the axion supermultiplet couples to QCD gauge fields via a high-dimensional interaction which leads to thermal production rates [12] depending on the reheat temperature T_R. Mixed axion/neutralino dark matter production in the SUSY KSVZ model has been computed in Ref's [13, 14, 15] for the case of suppressed saxion coupling to axions, and in Ref. [16] for unsuppressed couplings which lead to production of dark radiation from $s \to aa$ decay.[2]

In the SUSY DFSZ model, no exotic quark superfields are needed as the Higgs doublet superfields, H_u and H_d, are assumed to carry PQ charges. An attractive feature of the DFSZ model is that it provides a simple resolution of the so-called SUSY μ problem[21]: why is the superpotential μ term at the $m_{3/2}$ scale (as required by phenomenology) instead of as high as the (reduced) Planck scale $M_P \simeq 2 \times 10^{18}$ GeV, as expected for SUSY preserving terms? In the SUSY DFSZ model, the μ term is forbidden at tree-level by the PQ symmetry. However, a superpotential term such as

$$W \ni \lambda \frac{S^2}{M_P} H_u H_d \tag{1.2}$$

can be allowed. After the PQ symmetry breaking by a vacuum expectation value of the scalar component of S, $\langle S \rangle \sim f_a$, a mu term

$$\mu \sim \lambda f_a^2 / M_P \tag{1.3}$$

will be induced. The mu term is then at or around the weak scale for $f_a \sim 10^{10} - 10^{11}$ GeV assuming $\lambda \sim 1$.

The axion supermultiplet in DFSZ model couples directly to the Higgs fields with an interaction given by

$$\mathcal{L}_{\rm DFSZ} = \int d^2\theta (1 + B\theta^2) \mu e^{c_H A / v_{PQ}} H_u H_d, \tag{1.4}$$

where $1 + B\theta^2$ is a SUSY breaking spurion field and c_H is the PQ charge of the Higgs bilinear operator $H_u H_d$.

The production and decay channels of saxions and axinos are very different in the SUSY DFSZ case as compared to SUSY KSVZ. Due to the renormalizable DFSZ interactions, thermal production rates for axinos/saxions are independent of T_R. In addition, for given v_{PQ}, saxion and axino decay rates are larger and there are many more decay final states as compared to SUSY KSVZ. As a result, for comparable values of masses and f_a, the DFSZ saxion and axino are expected to be much shorter lived as compared to the KSVZ case.

Dark matter production in the SUSY DFSZ model has been considered previously. In Ref. [22, 23], the overall WIMP production scenario for SUSY DFSZ was portrayed. In Ref. [24], detailed calculations of axino production and decay were included. In the present work, we augment these previous studies by including further axino decay modes along with detailed computations of saxion decay rates. We examine not only thermal production of axinos but also thermal and non-thermal production of saxions. Finally, we account for

[2]Further references for dark radiation from SUSY axion models include [17, 18, 19, 20].

production of axions as well, which are necessarily present and add to the predicted dark matter abundance.

Our results also depend on which particular SUSY model spectrum is assumed. We introduce in Sec. 2 two SUSY benchmark models (the same points as in Ref. [16] for ease of comparison with the KSVZ case): one with a bino-like LSP and a standard overabundance of WIMP dark matter (SOA) and one with a Higgsino-like LSP (as motivated by recent naturalness studies [25]), which contains a standard underabundance of Higgsino-like WIMP dark matter (SUA). A concise summary of our results for the SUA case has been presented earlier in Ref. [26]; in the present work, we provide detailed discussion and formulae, and also consider the SOA case. In Sec. 3, we present simplified formulae for the saxion decay widths and exact leading order branching fractions and decay temperatures T_D^s. In Sec. 4 we present similar results for axino decays. In Sec. 5, we briefly discuss axion production and thermal axino and thermal/non-thermal saxion production rates. We evaluate under which conditions axinos or saxions can temporarily dominate the matter density of the universe. In Sec. 6, we examine several cosmological scenarios for the SUA and SOA benchmarks: 1. low ($f_a \sim 10^{10} - 10^{12}$ GeV), 2. medium ($f_a \sim 10^{12} - 10^{14}$ GeV), and 3. high ($f_a \sim 10^{14} - 10^{16}$ GeV) ranges of the PQ scale. While our SUA benchmark point easily lives in the low f_a regime, it can with trouble also be accommodated at medium and high f_a values. In contrast, the SOA benchmark fails to be viable at low or medium f_a, but can be viable at very high $f_a \gtrsim 10^{15}$ GeV under certain restrictions such as a low enough m_s value such that saxion decays to sparticles are kinematically disallowed. This latter point is especially important in that far higher f_a values can be accommodated in SUSY axion models than are usually considered from non-SUSY models: this is possible due to the capacity for large entropy dilution along with the usual possibility of a small initial axion misalignment angle [27]. In an Appendix, we list exact leading order saxion and axino decay formulae for the DFSZ SUSY axion model.

2. Two benchmark models for DFSZ SUSY study

In this Section, we summarize two SUSY model benchmark points which are useful for illustrating the dark matter production in the SUSY DFSZ axion model: one (labeled as SUA) has a standard thermal *underabundance* of neutralino cold dark matter (CDM) while the other (labeled as SOA) has a standard thermal *overabundance* of neutralinos.

The first point– listed as SUA– comes from *radiatively-driven natural SUSY* [25] with parameters from the 2-parameter non-universal Higgs model

$$(m_0,\ m_{1/2},\ A_0,\ \tan\beta) = (7025\text{ GeV},\ 568.3\text{ GeV},\ -11426.6\text{ GeV},\ 8.55) \tag{2.1}$$

with input parameters $(\mu,\ m_A) = (150,\ 1000)$ GeV. We generate the SUSY model spectra with Isajet 7.83 [28]. As shown in Table 1, with $m_{\tilde{g}} = 1.56$ TeV and $m_{\tilde{q}} \simeq 7$ TeV, it is safe from LHC searches. It has $m_h = 125$ GeV and a Higgsino-like neutralino with mass $m_{\widetilde{Z}_1} = 135.4$ GeV and standard thermal abundance from IsaReD [29] of $\Omega_{\widetilde{Z}_1}^{MSSM}h^2 = 0.01$, low by a factor ~ 10 from the measured dark matter density. Some relevant parameters,

	SUA (RNS2)	SOA (mSUGRA)
m_0	7025	3500
$m_{1/2}$	568.3	500
A_0	-11426.6	-7000
$\tan\beta$	8.55	10
μ	150	2598.1
m_A	1000	4284.2
m_h	125.0	125.0
$m_{\tilde{g}}$	1562	1312
$m_{\tilde{u}}$	7021	3612
$m_{\tilde{t}_1}$	1860	669
$m_{\widetilde{Z}_1}$	135.4	224.1
$\Omega^{\rm std}_{\widetilde{Z}_1}h^2$	0.01	6.8
$\sigma^{\rm SI}(\widetilde{Z}_1 p)$ pb	1.7×10^{-8}	1.6×10^{-12}

Table 1: Masses and parameters in GeV units for two benchmark points computed with ISAJET 7.83 and using $m_t = 173.2$ GeV.

masses and direct detection cross sections are listed in Table 1. It has very low electroweak finetuning.

For the SOA case, we adopt the mSUGRA/CMSSM model with parameters

$$(m_0,\ m_{1/2},\ A_0,\ \tan\beta,\ sign(\mu)) = (3500\ \text{GeV},\ 500\ \text{GeV},\ -7000\ \text{GeV},\ 10,\ +) \qquad (2.2)$$

The SOA point has $m_{\tilde{g}} = 1.3$ TeV and $m_{\tilde{q}} \simeq 3.6$ TeV, so it is just beyond current LHC sparticle search constraints. It is also consistent with the LHC Higgs discovery since $m_h = 125$ GeV. The lightest neutralino is mainly bino-like with $m_{\widetilde{Z}_1} = 224.1$ GeV, and the standard neutralino thermal abundance is found to be $\Omega^{\rm MSSM}_{\widetilde{Z}_1}h^2 = 6.8$, a factor of ~ 60 above the measured value [30]. Due to its heavy 3rd generation squark masses and large μ parameter, this point has very high electroweak finetuning [31].

3. Decay of saxion

In this section, we present simplified formulae for the partial decay widths of saxions. These widths play an essential role in determining the cosmic densities of mixed axion/neutralino cold dark matter. Since the saxion mixes with the CP-even Higgs bosons h and H, it has similar decay channels via a tiny mixing coupling proportional to $\sim \mu/f_a$. The couplings can be extracted by integrating Eq. (1.4). We list all the possible saxion decay channels in the following.

- $s \to hh\ /\ HH\ /\ hH\ /\ AA\ /\ H^+H^-$.

  The saxion decays to pairs of Higgs states arise from the saxion trilinear interaction as well as its mixing in Eq. (1.4). For a very heavy saxion, the mixing effect can be safely neglected and the partial decay widths, neglecting phase space factors (these

are included in the Appendix and also in all the numerical results) are approximately given by

$$\Gamma(s \to hh) \approx \frac{c_H^2}{16\pi}\frac{\mu^4}{v_{PQ}^2}\left(1 - \frac{m_A^2\cos^2\beta}{\mu^2}\right)^2 \frac{1}{m_s}, \tag{3.1}$$

$$\Gamma(s \to HH) \approx \frac{c_H^2}{16\pi}\frac{\mu^4}{v_{PQ}^2}\left(1 + \frac{m_A^2\cos^2\beta}{\mu^2}\right)^2 \frac{1}{m_s}, \tag{3.2}$$

$$\Gamma(s \to hH) \approx \frac{c_H^2}{32\pi}\left(\frac{m_A^2\cos\beta}{v_{PQ}}\right)^2 \frac{1}{m_s}, \tag{3.3}$$

$$\Gamma(s \to H^+H^-) \simeq 2\times\Gamma(s \to AA) \approx \frac{c_H^2}{8\pi}\frac{\mu^4}{v_{PQ}^2}\left(1 + \frac{m_A^2\cos^2\beta}{\mu^2}\right)^2 \frac{1}{m_s}. \tag{3.4}$$

Note that we take the limit of decoupling– $m_A^2 \gg m_h^2$ and large $\tan\beta \gg 1$– unless otherwise stated.

- $s \to ZZ \;/\; W^+W^- \;/\; ZA \;/\; W^+H^-$.

  These decay modes arise from the mixing between the saxion and Higgs states. For a heavy saxion, its decays into gauge boson states are dominated by the decays into Goldstone states and thus we can obtain similar approximate formulae as for the Higgs final states:

$$\Gamma(s \to W^+W^-) \simeq 2\times\Gamma(s \to ZZ) = \frac{c_H^2}{8\pi}\frac{\mu^4}{v_{PQ}^2}\left(1 - \frac{m_A^2\cos^2\beta}{\mu^2}\right)^2 \frac{1}{m_s}, \tag{3.5}$$

$$\Gamma(s \to W^+H^-) = \Gamma(s \to W^-H^+) \simeq \Gamma(s \to ZA) \approx \frac{c_H^2}{16\pi}\frac{m_A^4\cos^2\beta}{v_{PQ}^2}\frac{1}{m_s}. \tag{3.6}$$

- $s \to f\bar{f}$.

  These modes are obvious due to the saxion mixing with Higgs states and their couplings contain a suppression factor of m_f/v_{PQ}. Thus, the decay rate is expected to be very small compared to the above decay modes for generic parameter values with $m_f \ll \mu, m_A$. For the case of $s \to t\bar{t}$ decay, the decay rate is given by

$$\Gamma(s \to t\bar{t}) \approx \frac{N_c}{4\pi}\frac{c_H^2 m_t^2}{v_{PQ}^2}\frac{\mu^4}{m_s^3}\left(1 - \frac{m_A^2\cos^2\beta}{2\mu^2}\right)^2. \tag{3.7}$$

- $s \to \widetilde{Z}_i\widetilde{Z}_j \;/\; \widetilde{W}_i\widetilde{W}_j$.

  In the heavy saxion limit, $m_s \gg \mu$, the saxion decays dominantly to Higgsino-like neutralinos and charginos whose partial decay widths are given by

$$\Gamma(s \to \text{all neutralinos}) \approx \frac{c_H^2}{64\pi}\left(\frac{\mu}{v_{PQ}}\right)^2 m_s, \tag{3.8}$$

$$\Gamma(s \to \text{all charginos}) \approx \frac{c_H^2}{64\pi}\left(\frac{\mu}{v_{PQ}}\right)^2 m_s. \tag{3.9}$$

- $s \to \tilde{f}\tilde{f}$.

  Similarly to fermion modes, these decay rates are also expected to be very small due to the Yukawa suppression. For the case of $s \to \tilde{t}_1\tilde{t}_1$,

$$\Gamma(s \to \tilde{t}_1\tilde{t}_1) \approx \frac{N_c}{2\pi}\frac{c_H^2\mu^4}{v_{PQ}^2}\frac{m_t^4}{m_s^5}\left(1 - \frac{m_A^2\cos^2\beta}{2\mu^2}\right)^2. \tag{3.10}$$

  Note that we neglect the squark mixing effect which is not very large for our benchmark points.

- $s \to aa$ / $\tilde{a}\tilde{a}$.

  Finally, the saxion has generic trilinear couplings to axions and axinos which depend on the details of PQ symmetry breaking sector. The partial decay widths are given by

$$\Gamma(s \to aa) = \frac{\xi^2 m_s^3}{64\pi v_{PQ}^2}, \tag{3.11}$$

$$\Gamma(s \to \tilde{a}\tilde{a}) = \frac{\xi^2}{8\pi}\frac{m_{\tilde{a}}^2 m_s}{v_{PQ}^2}\left(1 - 4\frac{m_{\tilde{a}}^2}{m_s^2}\right)^{3/2}. \tag{3.12}$$

  Here the model dependent parameter $\xi \lesssim 1$ quantifies the axion superfield trilinear coupling.

In the following, we will show explicit numerical examples of saxion decays into the aforementioned final states. We can see the relative ratios of such decay modes for the SUA and SOA benchmark points and for $\xi = 0$ or 1.

3.1 Saxion branching fractions

Fig. 1 shows saxion branching ratios (BR) versus m_s for the case of $\xi = 0$ (for which there are no decays into axion or axino pairs) for *a*) the SUA case and *b*) the SOA case. We take $f_a = 10^{12}$ GeV. For $\xi = 0$ and a large saxion mass in the SUA case, the most important decays are into SUSY particles: charginos and neutralinos (the curves nearly overlap). Decays into gauge and Higgs particles are subdominant– about one or two orders of magnitude smaller than the neutralino and chargino modes for multi-TeV values of m_s. This behavior can be understood from the approximate formulae, Eqs. (3.1)-(3.9). The partial decay widths are proportional to m_s for the decay to neutralinos and charginos while they are inversely proportional to m_s for the decays into gauge and Higgs states. For smaller saxion mass, *e.g.* $m_s \lesssim 1.5$ TeV, the decay into top quark pairs also becomes sizable. Note that the decays into gauge and Higgs states are strongly suppressed for the saxion mass around 1 TeV for which the saxion-Higgs mixing is maximized so that the saxion coupling to gauge and Higgs particles become very small due to cancellation.

In frame *b*) we show the case for the SOA benchmark. Here, the dominant decay modes are instead into gauge boson and Higgs final states. This behavior arises because

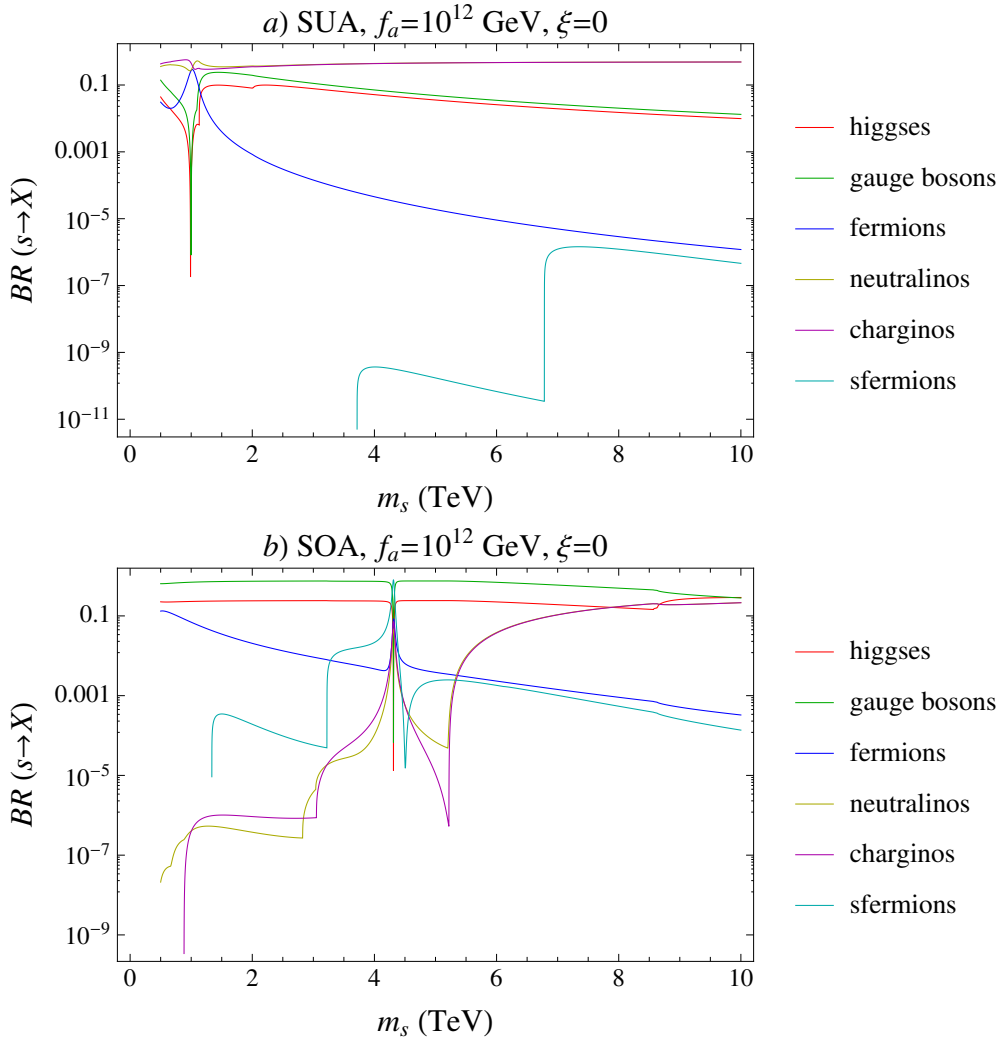

Figure 1: Saxion decay branching ratios for $f_a = 10^{12}$ GeV and $\xi = 0$ for *a*) SUA and *b*) SOA benchmark points.

for the SOA case $\mu \simeq 2.6$ TeV which is quite large. From Eq's (3.1)-(3.6), we can see that these partial widths are proportional to μ^4 instead of μ^2 as per the decay to -inos.

In Fig. 2, we show the saxion BRs for $\xi = 1$, assuming $m_{\tilde{a}} = 2$ TeV. In the case of SUA, the most important mode is $s \to aa$ where the BR is a few orders of magnitude larger than other MSSM modes including those to sparticles and SM particles for a large saxion mass. This can be understood since the decay into axion pairs is proportional to m_s^3 while the others are proportional to m_s or $1/m_s$. When the saxion mass is much larger than the SUSY particle masses– *i.e.* for saxion mass around 10 TeV– $BR(s \to \text{SM})$ is smaller than 10^{-3} and thus the constraint from dark radiation becomes stronger if saxions dominate the energy density of the universe. Also, if $s \to \tilde{a}\tilde{a}$ is allowed, then it might become the dominant source of neutralino dark matter via the axino decay.

For smaller saxion mass, $m_s \lesssim 1$ TeV, the BRs of the MSSM channels become larger

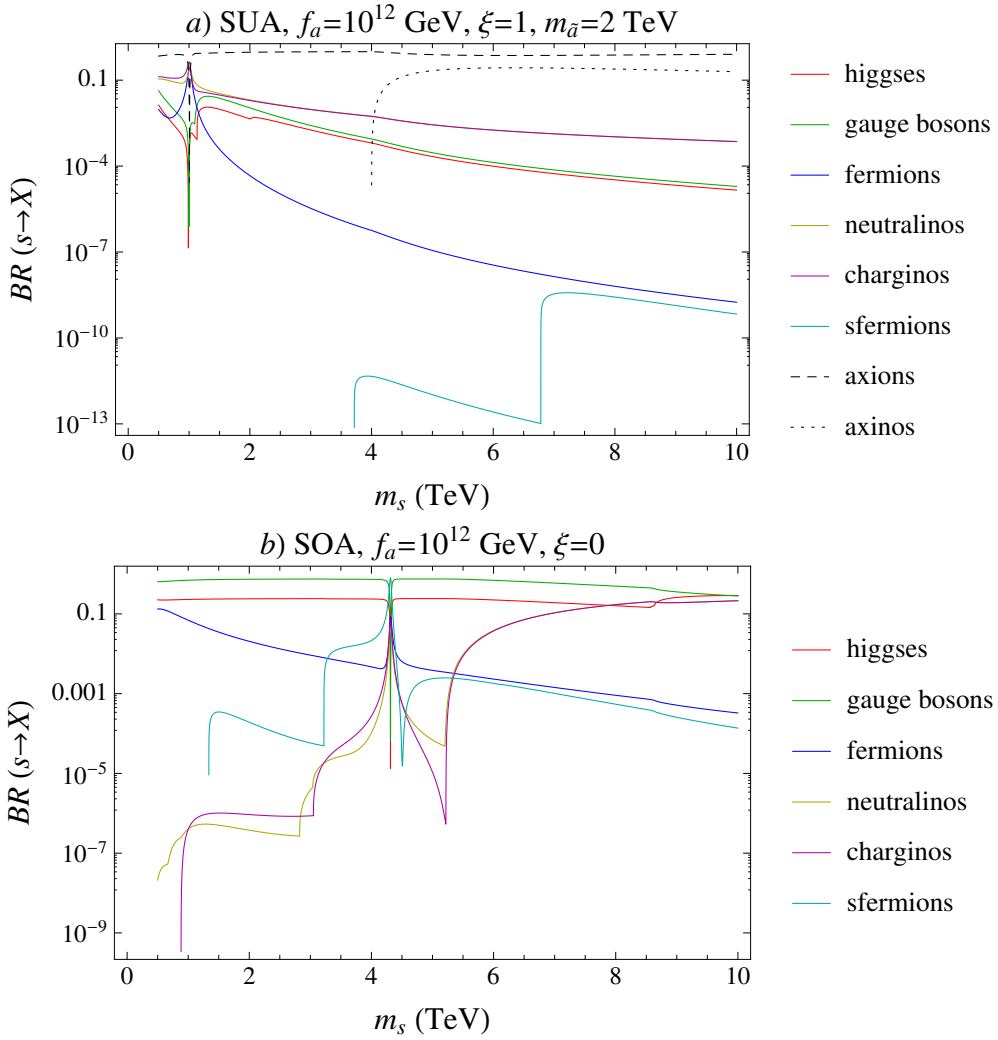

Figure 2: Saxion branching ratios for $f_a = 10^{12}$ GeV and $\xi = 1$ for *a*) SUA and *b*) SOA benchmark points. Here we take $m_{\tilde{a}} = 2$ TeV to show saxion decay into axino pair.

so that the constraint from dark radiation becomes relieved. The saxion mass around 1 TeV shows an interesting behavior in that the neutralino/chargino modes become sizable and thus the amount of dark radiation from saxion decay can be drastically reduced.

In frame *b*), we show the $\xi = 1$ case for the SOA benchmark. For large $m_s \gtrsim 4.3$ TeV, the $s \to aa$ mode is again dominant. It is worth noting that the decay widths to neutralinos and charginos never becomes larger than the Higgs and gauge boson modes for $m_s \lesssim 10$ TeV in contrast to the SUA case. Thus, augmentation of neutralino dark matter via late decay of saxions can not be very large, which will be discussed in detail in Sec. 5. For $m_s \lesssim 8^{1/4}\mu \simeq 4.3$ GeV, the dominant final state is into SM particles; thus, in this case, low rates of dark radiation occur even when saxions dominate the universe. We will discuss this in Section 6. For $m_s \simeq m_A$, mixing between saxions and Higgses becomes very large so that the sfermion final states become the dominant decay modes.

3.2 Saxion decay temperature

In this subsection, we show saxion decay temperature values expected from the SUA and SOA benchmarks for $\xi = 0$ and 1. The temperature at which saxions decay is related to the total decay width via

$$T_D = \sqrt{\Gamma M_P}/(\pi^2 g_*(T_D)/90)^{1/4} \tag{3.13}$$

where M_P is the reduced Planck mass and g_* is the effective number of degrees of freedom at temperature T_D. Note that we assume a radiation-dominated universe in the temperature plots. The case of a saxion-dominated universe will be discussed in Sec. 5.

In Fig. 3, we show the saxion decay temperature for $f_a = 10^{10}$, 10^{12} and 10^{14} GeV. For the $\xi = 0$ case shown in frame *a*), $T_D^s \sim 10$ MeV for $f_a \sim 10^{14}$ GeV so that even for these large values of f_a, the saxion decays before the onset of BBN. For $f_a \sim 10^{10}$ GeV, the decay temperature typically ranges up to 100 GeV. This is typically well above WIMP freezeout temperature, given approximately by $T_{fr} \sim m_{\widetilde{Z}_1}/25$. Thus, for low f_a, saxions in the DFSZ model tend to decay before freezeout, and so the standard thermal WIMP abundance calculation may remain valid.

In the SOA case shown in frame *b*), T_D^s varies from $1 - 10^4$ GeV as f_a ranges from $10^{14} - 10^{10}$ GeV. Thus, saxions tend to decay well before WIMP freezeout unless f_a is as large as 10^{14} GeV, in which case saxion decays are suppressed.

In Fig. 4, we show the saxion decay temperature for $\xi = 1$. In frame *a*) for the SUA case, and with $m_{\tilde{a}} = 2$ TeV, the presence of the $s \to aa, \tilde{a}\tilde{a}$ modes increases even further the saxion decay temperature compared to the $\xi = 0$ case. For $m_s = 10$ TeV, we see that T_D^s ranges from $1 - 10^4$ GeV as $f_a \sim 10^{14} - 10^{10}$ GeV. In frame *b*), we find a similar decay temperature for SOA as compared to SUA since T_D^s is dominated by the $s \to aa,\ \tilde{a}\tilde{a}$ widths which are the same for both cases.

The upshot of this section is that in the DFSZ model, direct coupling of saxions to Higgs and Higgsinos increases the saxion decay widths compared to the KSVZ model, typically causing saxions to decay before the BBN onset even for f_a as large as 10^{14} GeV, and for smaller f_a values, saxions tend to decay even before neutralino freezeout, thus leading to no augmentation of neutralino relic density via late-time reannihilation.

4. Axino decays

Similar to the saxion case, the axino trilinear couplings arise directly or indirectly through the axino-Higgsino mixing from the superpotental (1.4). The possible decay modes include the following.

- $\tilde{a} \to \widetilde{Z}_i h \ / \ \widetilde{Z}_i H \ / \ \widetilde{Z}_i A$.

  The decays into neutralinos and Higgs bosons come from the axino-Higgsino-Higgs interaction, so the dominant decay modes are into Higgsino-like neutralino states in the limit of heavy axino. In the heavy axino limit (*i.e.* $m_{\tilde{a}} \gg \mu$), the partial decay width is given by

$$\Gamma(\tilde{a} \to \widetilde{Z}_i \phi) \approx 2 \times 3 \times \frac{c_H^2}{64\pi} \left(\frac{\mu}{v_{PQ}}\right)^2 m_{\tilde{a}}. \tag{4.1}$$

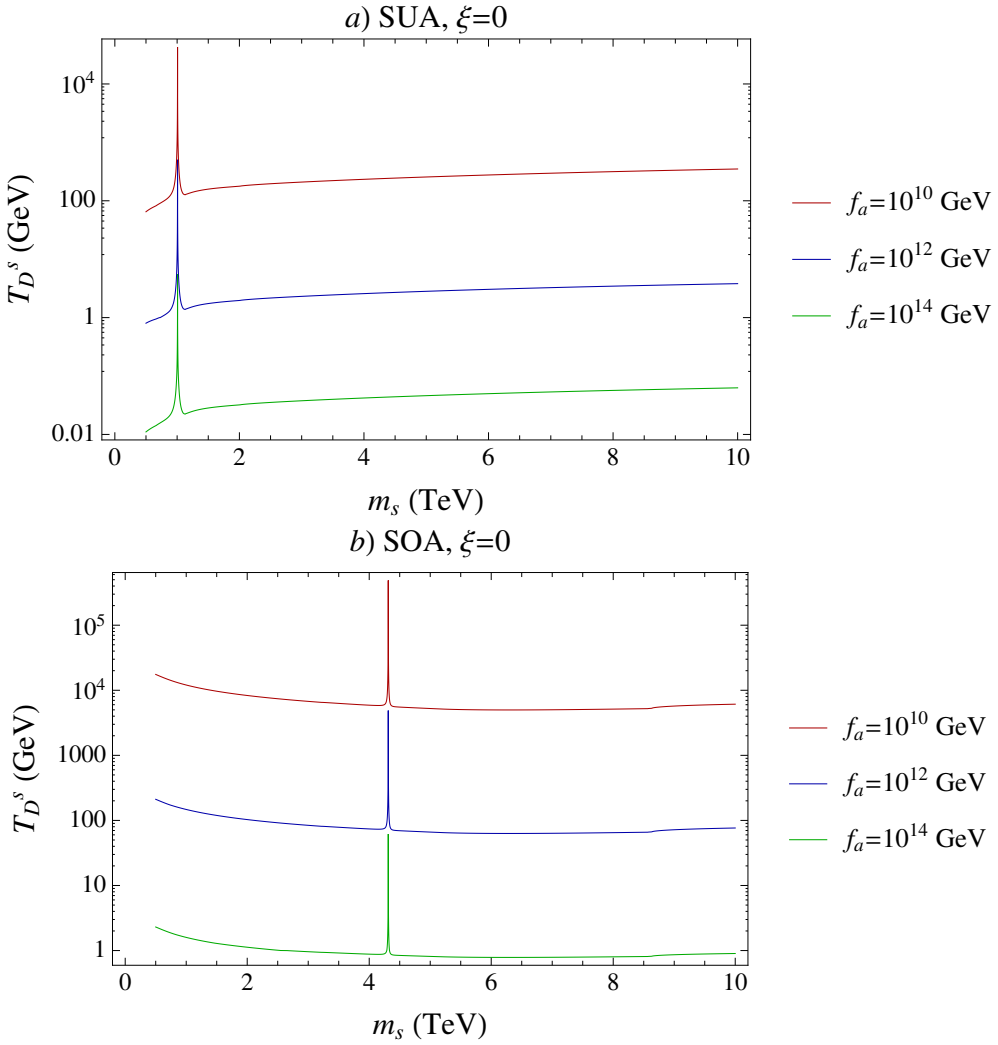

Figure 3: Saxion decay temperature for $f_a = 10^{12}$ GeV and $\xi = 0$ for *a*) SUA and *b*) SOA benchmark points.

where $\phi = h,\ H$ and A.

- $\tilde{a} \to \widetilde{W}_i^{\pm} H^{\mp}$.

  These decay modes arise similarly to the previous ones. For the heavy axino limit, the partial width is determined by

$$\Gamma(\tilde{a} \to \widetilde{W}_i^{\pm} H^{\mp}) \approx \frac{c_H^2}{16\pi} \left(\frac{\mu}{v_{PQ}}\right)^2 m_{\tilde{a}}. \tag{4.2}$$

- $\tilde{a} \to \widetilde{Z}_i Z \ /\ \widetilde{W}_i^{\pm} W^{\mp}$.

  The axino decays to gauge bosons arise from the axino-neutralino mixing. In the limit of heavy axino, the corresponding decay rates can be obtained by considering

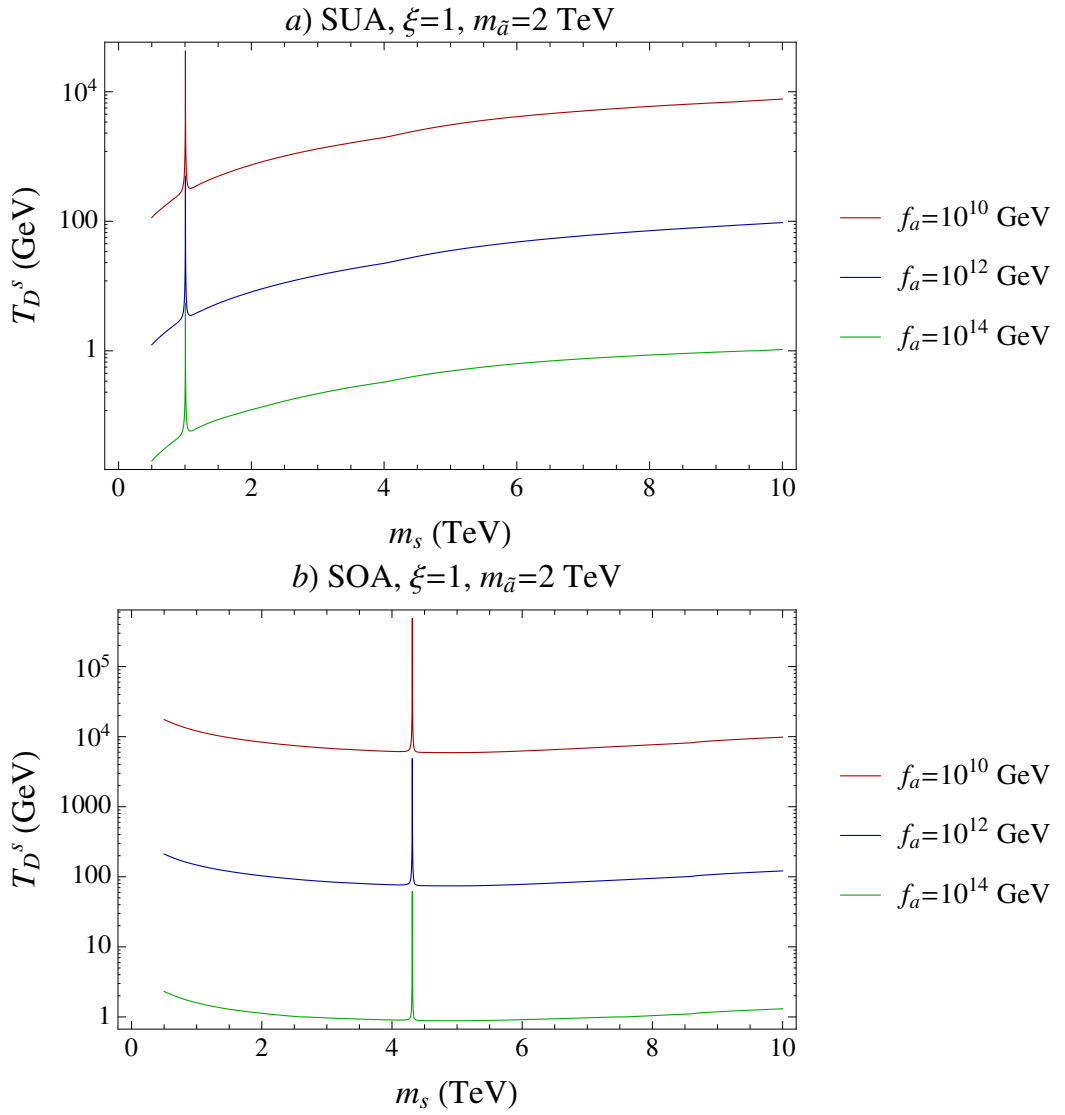

Figure 4: Decay temperature for saxion with $f_a = 10^{12}$ GeV, $\xi = 1$ and $m_{\tilde{a}} = 2$ TeV for *a*) SUA and *b*) SOA benchmark points.

the decays into the Goldstone modes as follows:

$$\Gamma(\tilde{a} \to \widetilde{Z}_i Z\ ) \approx \frac{c_H^2}{32\pi}\left(\frac{\mu}{v_{PQ}}\right)^2 m_{\tilde{a}}, \tag{4.3}$$

$$\Gamma(\tilde{a} \to \widetilde{W}_i^{\pm} W^{\mp}) \approx \frac{c_H^2}{16\pi}\left(\frac{\mu}{v_{PQ}}\right)^2 m_{\tilde{a}}. \tag{4.4}$$

- $\tilde{a} \to \tilde{f} f$.

  These modes also arise from axino-neutralino mixing. In most cases, they are suppressed by m_f/v_{PQ} as in the saxion case, and kinematically disallowed in most of

parameter space with heavy matter scalars. For the case of $\tilde{a} \to \tilde{t}_1 \bar{t} + \text{c.c.}$,

$$\Gamma(\tilde{a} \to \tilde{t}_1 \bar{t} + \bar{\tilde{t}}_1 t) \approx \frac{N_c}{32\pi} \frac{c_H^2 \mu^4}{v_{PQ}^2} \frac{m_t^2}{m_{\tilde{a}}^3} \left(1 + \frac{m_{\tilde{a}}}{\mu \tan\beta}\right)^2 . \tag{4.5}$$

Note that we neglect the mixing effect of stop as in the case of $s \to \tilde{t}_1 \tilde{t}_1$.

4.1 Axino branching fractions

In the Fig. 5, we show the axino branching fractions as a function of $m_{\tilde{a}}$ for a) the SUA and b) the SOA benchmark points. In most of parameter space, the branching fractions for decay to neutralino+neutral Higgs, chargino+charged Higgs, neutralino+Z and chargino+W are all comparable, in the tens of percent, while decays to fermion+sfermion are suppressed. This is consistent with the above discussion and approximate formulae except for the region of $m_{\tilde{a}} \sim m_{\widetilde{Z}_i}$ for which axino-neutralino mixing is enhanced. For the SOA case, the qualitative features for large $m_{\tilde{a}}$ are almost the same as SUA case. The differences come only from the different particle mass spectrum. For $m_A \simeq \mu = 2.6$ TeV, we can see the effect of maximized axino-Higgsino mixing leading to the domination of the sfermion plus fermion mode.

4.2 Axino decay temperature

In Fig. 6, we show the axino decay temperature $T_D^{\tilde{a}}$ versus $m_{\tilde{a}}$ for a) the SUA and b) the SOA benchmarks, for $f_a = 10^{10}$, 10^{12} and 10^{14} GeV. In SUA case, we see that $T_D^{\tilde{a}}$ varies from $\mathcal{O}(10)$ MeV to $\mathcal{O}(100)$ GeV depending on the f_a value. Since the axino always decays to SUSY particles, it should always augment the neutralino abundance unless $T_D^{\tilde{a}} > T_{fr}$, in which case the usual thermal abundance applies, unless affected by saxion decays. One typically has $T_D^{\tilde{a}} > T_{fr}$ as long as $f_a \lesssim 10^{11}$ GeV. For the SOA case with a large $\mu = 2.6$ GeV, $T_D^{\tilde{a}}$ is about an order of magnitude higher than for the SUA case.

5. Axion, axino and saxion production in the SUSY DFSZ model

In this section, we will present formulae for the axion, axino and saxion production, and discuss the possibility of saxion or axino domination in the early universe.

5.1 Axion production

Here we will assume the scenario where the PQ symmetry breaks before the end of inflation, so that a nearly uniform value of the axion field $\theta_i \equiv a(x)/f_a$ is expected throughout the universe. From the axion equation of motion, the axion field stays relatively constant until temperatures approach the QCD scale $T_{\rm QCD} \sim 1$ GeV. At this point, a temperature-dependent axion mass term turns on, and a potential is induced for the axion field. At temperature T_a the axion field begins to oscillate, filling the universe with low energy (cold) axions. The standard axion relic density (via this vacuum misalignment mechanism) is derived assuming that coherent oscillations begin in a radiation-dominated universe and is given by [9, 10]

$$\Omega_a^{\rm std} h^2 \simeq 0.23 f(\theta_i) \theta_i^2 \left(\frac{f_a/N}{10^{12}\ \text{GeV}}\right)^{7/6} \tag{5.1}$$

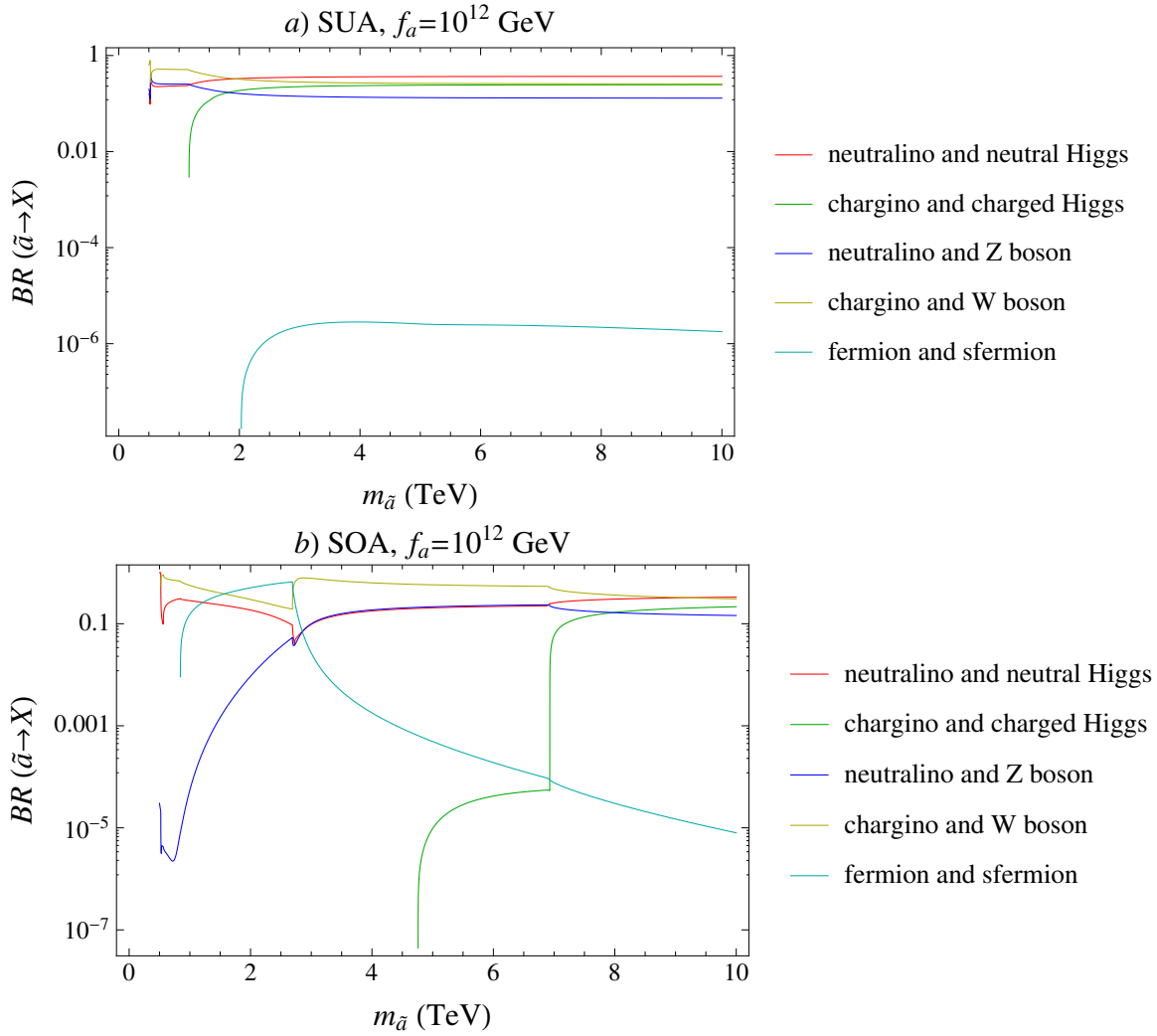

Figure 5: Axino branching ratios for $f_a = 10^{12}$ GeV and for *a*) SUA and *b*) SOA benchmark points.

where $0 < \theta_i < \pi$ and $f(\theta_i)$ is the anharmonicity factor. Visinelli and Gondolo [10] parameterize the latter as $f(\theta_i) = \left[\ln\left(\frac{e}{1-\theta_i^2/\pi^2}\right)\right]^{7/6}$. The uncertainty in $\Omega_a h^2$ from vacuum misalignment is estimated as plus-or-minus a factor of three. If the axion field starts to oscillate during the matter dominated (MD) or the decaying particle dominated (DD) phase ($T_D < T_a < T_e$), the axion relic density will no longer be given by Eq. (5.1). The appropriate expressions for each of these cases are given in the Appendix of Ref. [14].

5.2 Axino and saxion production

In the case of the KSVZ models, thermal production of saxions and axinos is due to the

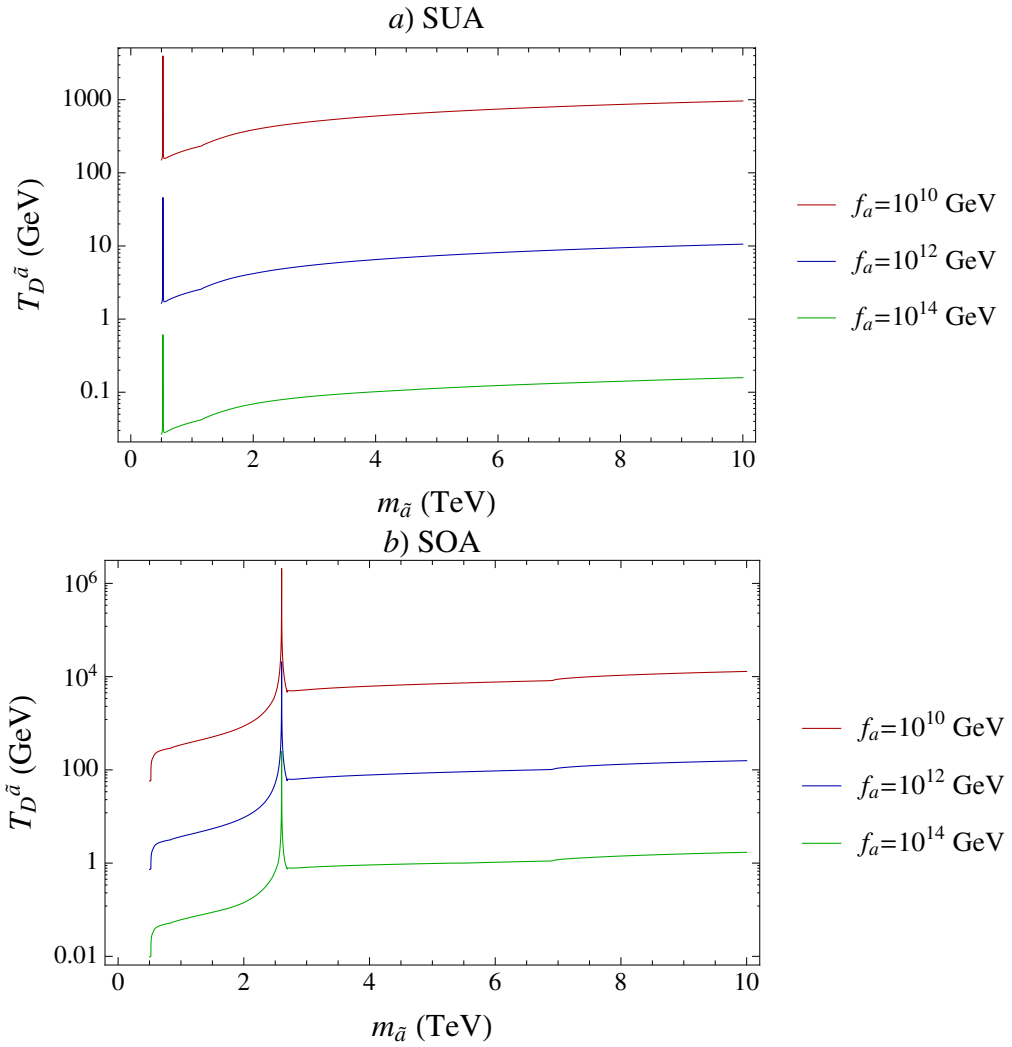

Figure 6: Axino decay temperature for $f_a = 10^{12}$ GeV and for *a*) SUA and *b*) SOA benchmark points.

anomaly interaction of dimension 5:

$$\begin{aligned}\mathcal{L}_{\text{anomaly}} &= -\frac{\sqrt{2}\alpha_s}{8\pi f_a}\int d^2\theta A W^a W^a + \text{h.c.} \\ &= \frac{\alpha_s}{8\pi f_a}\left(sG^a_{\mu\nu}G^{a\mu\nu} - i\bar{\tilde{a}}\frac{[\gamma^\mu,\gamma^\nu]}{2}\gamma_5\tilde{g}^a G^a_{\mu\nu} + \cdots\right). \end{aligned} \tag{5.2}$$

This higher dimensional couplings lead to thermally produced saxion and axino densities which are proportional to the reheat temperature T_R.

In contrast, the axion supermultiplet in the SUSY DFSZ model has Yukawa-type (dimension 4) interactions as shown in Eq. (1.4). As a consequence, the most important contributions for the saxion and axino production arise near the kinematic thresholds of scattering processes leading to thermal production densities which are independent of T_R

so long as T_R is larger than the kinematic threshold for the specific process. As was studied in Ref's [22, 23, 24], the saxion and axino abundances from thermal production are given by

$$Y_s^{\rm TP} = 10^{-7}\zeta_s \left(\frac{B\mu/\mu \text{ or } \mu}{\rm TeV}\right)^2 \left(\frac{10^{12}\ {\rm GeV}}{f_a}\right)^2, \tag{5.3}$$

$$Y_{\tilde{a}}^{\rm TP} = 10^{-7}\zeta_{\tilde{a}} \left(\frac{\mu}{\rm TeV}\right)^2 \left(\frac{10^{12}\ {\rm GeV}}{f_a}\right)^2, \tag{5.4}$$

where ζ_s and $\zeta_{\tilde{a}}$ are model-dependent constants of order unity. [3] Barring a specific model-dependence on ζ_s and $\zeta_{\tilde{a}}$, we will now examine the possibility of having a cosmological era dominated by thermally produced saxions or axinos. For this, we need to compare two important quantities; the decay temperature T_D and the saxion/axino-radiation equality temperature T_e.

Let us first discuss the saxion case. The saxion-radiation equality temperature is given by

$$T_e^s = \frac{4}{3} m_s Y_s^{\rm TP} = \frac{4}{3}\times 10^{-7}\zeta_s \left(\frac{B\mu/\mu \text{ or } \mu}{\rm TeV}\right)^2 \left(\frac{10^{12}\ {\rm GeV}}{f_a}\right)^2 m_s, \tag{5.5}$$

and the decay temperature is

$$T_D^s = \sqrt{\Gamma_s M_p}\left(\frac{90}{\pi^2 g_*}\right)^{1/4}. \tag{5.6}$$

The saxion decay width is approximately given by

$$\Gamma_s \approx \frac{c_H^2}{32\pi}\left(\frac{\mu}{v_{PQ}}\right)^2 m_s = \frac{c_H^2}{16\pi}\left(\frac{\mu}{f_a}\right)^2 m_s. \tag{5.7}$$

Here we only consider the decay width for $\xi = 0$ and the dominant decays into neutralinos and charginos for the SUA scenario. For the case of SOA, the situation does not significantly change. The condition for the saxion domination, $T_e^s > T_D^s$, leads to

$$\frac{(B\mu/\mu \text{ or } \mu)^2/\mu}{f_a} \gtrsim 3\times 10^{-5}\left(\frac{c_H}{\zeta_s}\right)\left(\frac{90}{g_*}\right)^{1/4}\left(\frac{\rm TeV}{m_s}\right)^{1/2}. \tag{5.8}$$

This condition is hardly achieved for $f_a \gtrsim 10^9$ GeV unless $B\mu/\mu$ or μ is as large as 100 TeV. Thus, we conclude that the saxion domination is unlikely to occur in the case of thermal production. If $\xi \neq 0$, the saxion decay temperature becomes larger, and thus the saxion domination is even less probable. The same conclusion can be drawn for the axino case where the axino domination requires

$$\frac{\mu}{f_a} \gtrsim 8\times 10^{-5}\left(\frac{c_H}{\zeta_{\tilde{a}}}\right)\left(\frac{90}{g_*}\right)^{1/4}\left(\frac{\rm TeV}{m_{\tilde{a}}}\right)^{1/2} \tag{5.9}$$

which is also hard to meet.

[3] For numerical discussion in Sec. 6, we take $\xi_s = \xi_{\tilde{a}} = 1$ and $\max[B\mu/\mu, \mu]$.

Next we consider saxion coherent oscillations. In this case, the saxion abundance is given by

$$Y_s^{\rm CO} = 1.9 \times 10^{-6} \left(\frac{\rm GeV}{m_s}\right) \left(\frac{\min[T_R, T_s]}{10^7\ {\rm GeV}}\right) \left(\frac{f_a}{10^{12}\ {\rm GeV}}\right)^2 \tag{5.10}$$

assuming an initial saxion field amplitude of $s_0 = f_a$. From this, one finds that the saxion domination occurs for

$$f_a \gtrsim 8 \times 10^{13}\ {\rm GeV} \times c_H^{1/3} \left(\frac{90}{g_*}\right)^{1/12} \left(\frac{10^7\ {\rm GeV}}{\min[T_R, T_s]}\right)^{1/3} \left(\frac{\mu}{150\ {\rm GeV}}\right)^{1/3} \left(\frac{m_s}{5{\rm TeV}}\right)^{1/6}. \tag{5.11}$$

Note that the lower limit on f_a becomes larger for smaller T_R or T_s.

For illustration, the various temperatures are shown as a function of f_a for $\xi = 0$ in Fig. 7 for *a*) the SUA benchmark and in *b*) for the SOA benchmark. We take $m_s = m_{\tilde{a}} = 5$ TeV for SUA and $m_s = m_{\tilde{a}} = 500$ GeV for SOA. For low $f_a \lesssim 10^{12-13}$ GeV, saxions and axinos decay before the neutralino freeze-out when the universe is radiation-dominated in which case the neutralino dark matter density is determined by the usual freeze-out mechanism. For 10^{12} GeV$\lesssim f_a \lesssim 10^{14}$ GeV, saxions and axinos decay after neutralino freeze-out so that the neutralino re-annihilation process becomes important to determine the WIMP portion of the dark matter density. For $f_a \gtrsim 10^{14}$ GeV, saxion coherent oscillation can dominate over radiation and the saxion decay occurs after neutralino freeze-out. In this case, the WIMP abundance may be depleted by late-time entropy injection, or augmented if saxions decay at a large rate into SUSY particles.

The case for $\xi = 1$ is shown in Fig. 8. For $\xi = 1$, the decay $s \to aa$ (and possibly $s \to \tilde{a}\tilde{a}$) is allowed, which leads to an even earlier saxion decay, but also to the possible production of dark radiation. Since the saxion decay temperature is even higher than the $\xi = 0$ case, the equality occurs when f_a is a few times larger than the $\xi = 0$ case.

We are now ready to make a detailed study of several cosmological scenarios of the SUSY DSFZ model.

6. Cosmological scenarios depending on f_a

In this section, we will discuss various cosmological scenarios which have different characteristics depending on the PQ scale f_a ($= \sqrt{2} v_{PQ}$). Our analysis will be presented separately for SUA and SOA.

6.1 SUA

As was discussed previously with Figs. 7*a*) and 8*a*), there are three regions of f_a having different cosmological properties in terms of the dark matter abundance: 1. $f_a \lesssim 10^{12}$ GeV, 2. 10^{12} GeV$\lesssim f_a \lesssim 10^{14}$ GeV and 3. $f_a \gtrsim 10^{14}$ GeV for which saxions (axinos) decay 1. before dark matter freeze-out 2. after freeze-out and 3. dominate the universe before their decay.

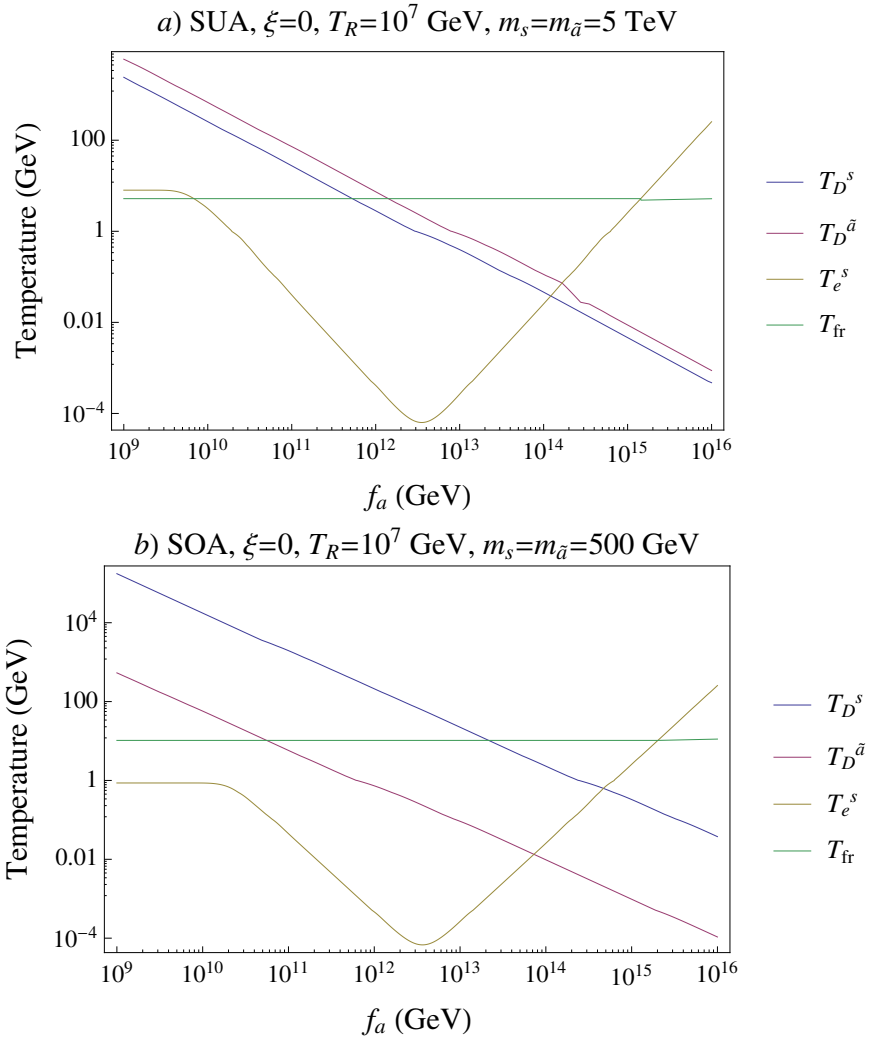

Figure 7: Saxion (blue) and axino (purple) decay temperature along with saxion-radiation equality temperature (green) are shown for *a*) the SUA and *b*) the SOA benchmark point for $\xi = 0$. The neutralino freeze-out temperature is also shown. We use $T_R = 10^7$ GeV and $m_s = m_{\tilde{a}} = 5$ TeV for *a*) and $m_s = m_{\tilde{a}} = 0.5$ TeV for *b*).

6.1.1 $f_a \lesssim 10^{12}$ GeV

In this region, axinos and saxions are produced mainly by thermal scattering and thus they do not dominate the universe. Furthermore, they decay before neutralino freeze-out so that the standard thermal relic density $\Omega^{\rm std}_{\tilde{Z}_1}h^2 = 0.01$ remains valid. In this region, then, the main component of dark matter would come from misalignment-produced cold axions. The initial misalignment angle θ_i can always be adjusted so that $\Omega_a h^2 = 0.12 - \Omega_{\tilde{Z}_1}h^2$. Thus, for $f_a \lesssim 10^{12}$ GeV, we would expect in the SUA benchmark case a universe with dark matter at $\sim 10\%$ Higgsino-like WIMPs along with 90% cold axions[26].

It remains to check how sizable is the relativistic axion production from the saxion decay or thermal scattering. The effective number of neutrinos from relativistic axions is

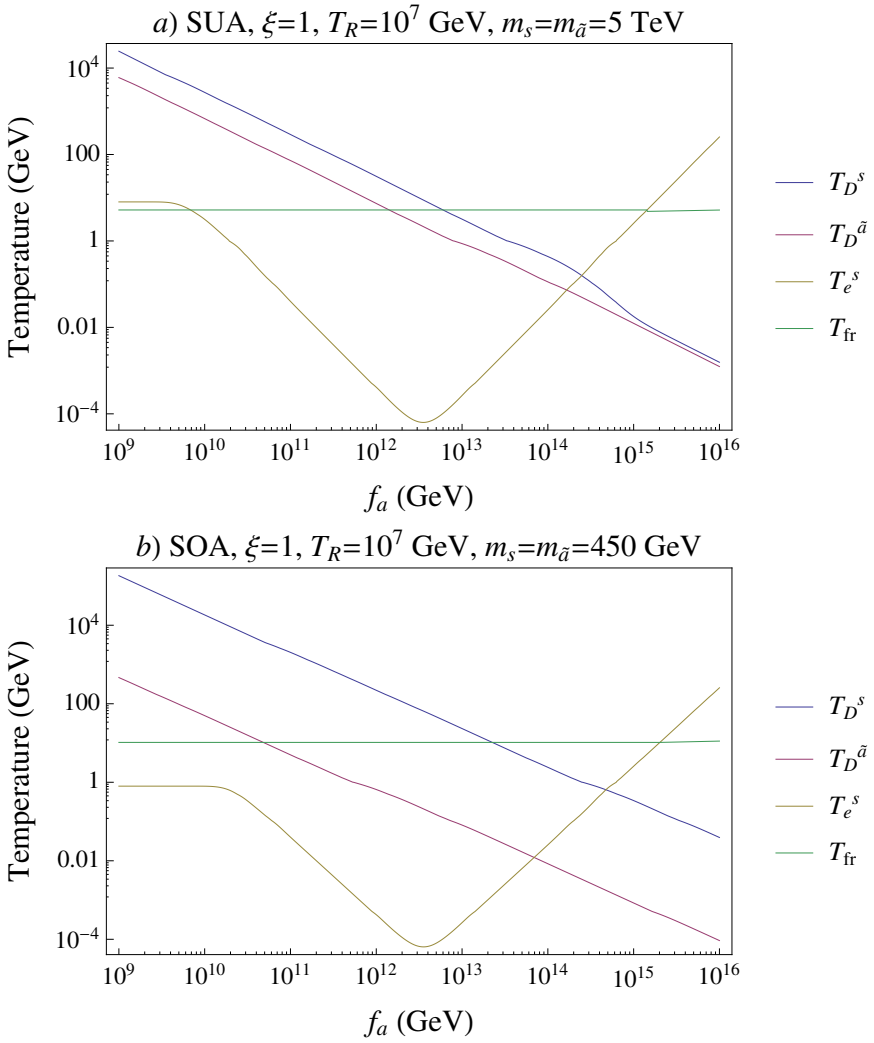

Figure 8: Saxion (blue) and axino (purple) decay temperature along with saxion-radiation equality temperature (green) are shown for *a*) the SUA and *b*) the SOA benchmark point for $\xi = 1$. The neutralino freeze-out temperature is also shown. We use $T_R = 10^7$ GeV and $m_s = m_{\tilde{a}} = 5$ TeV for *a*) and $m_s = m_{\tilde{a}} = 0.5$ TeV for *b*).

given by

$$\Delta N_{\rm eff} \simeq \Delta N_{\rm eff}^{\rm TP} + \frac{18}{r} BR(s \to aa) g_{*S}(T_D)^{-1/3} \frac{m_s \left(Y_s^{\rm CO} + Y_s^{\rm TP}\right)}{T_D^s} \tag{6.1}$$

where r is the factor of entropy dilution. In this region there is no entropy dilution ($r = 1$). In most cases, thermal production of axions is negligible and thus it is enough to only take the saxion decay into account. The most important quantity is $BR(s \to aa)$ which was discussed in Sec. 3. For $m_s \gtrsim 4$ TeV, the dominant decay mode of the saxion is its decay

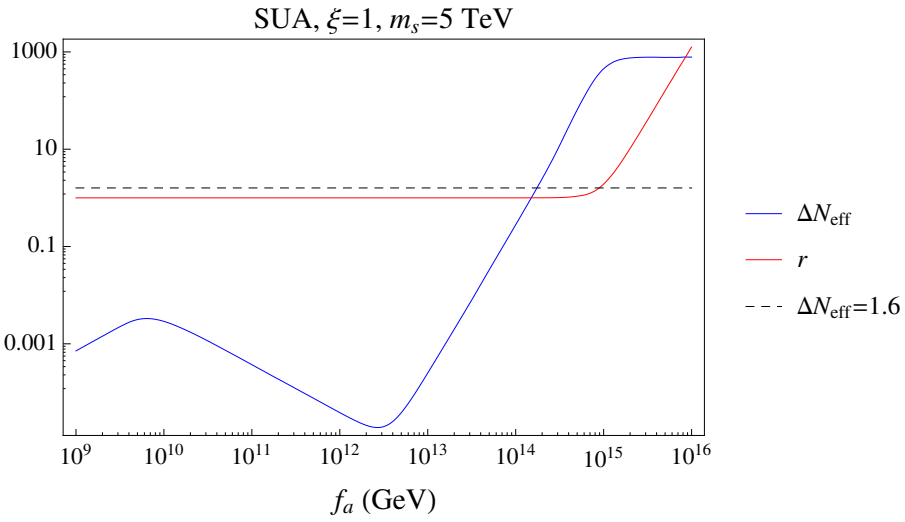

Figure 9: Plot for $\Delta N_{\rm eff}$ and r in SUA, $\xi = 1$ and $m_s = 5$ TeV.

to neutralinos and charginos. Thus, we get to a good approximation,

$$\begin{aligned} BR(s \to aa) &\approx \frac{\Gamma(s \to aa)}{\Gamma\left(s \to \widetilde{Z}\widetilde{Z}\right) + \Gamma\left(s \to \widetilde{W}\widetilde{W}\right) + \Gamma(s \to aa)} \\ &\approx \frac{\xi^2 m_s^3/(32\pi f_a^2)}{c_H^2 \mu^2 m_s/(16\pi f_a^2) + \xi^2 m_s^2/(32\pi f_a^2)} \\ &= \frac{\xi^2 m_s^2}{2c_H^2\mu^2 + \xi^2 m_s^2} \end{aligned} \tag{6.2}$$

which leads to

$$\begin{aligned} \Delta N_{\rm eff} &\simeq 18 \times g_{*S}(T_D)^{-1/3} \frac{\xi^2 m_s^2}{2c_H^2\mu^2 + \xi^2 m_s^2} \frac{m_s Y_s^{\rm TP}}{T_D^s} \\ &\approx 6.6 \times 10^{-5} \left(1 + \frac{2c_H^2\mu^2}{\xi^2 m_s^2}\right)^{-3/2} \left(\frac{\zeta_s}{\xi}\right) \left(\frac{g_{*S}}{90}\right)^{-1/3} \left(\frac{g_*}{90}\right)^{1/4} \\ &\quad \times \left(\frac{5\ \text{TeV}}{m_s}\right)^{1/2} \left(\frac{B\mu/\mu\ \text{or}\ \mu}{\text{TeV}}\right)^2 \left(\frac{10^{12}\ \text{GeV}}{f_a}\right). \end{aligned} \tag{6.3}$$

In the range of 10^{10} GeV$\lesssim f_a \lesssim 10^{12}$ GeV, one finds $\Delta N_{\rm eff}$ typically between 10^{-3} and 10^{-5} even with $\xi = 1$ as can be seen clearly from Fig. 9. Note also that the saxion density approaches its equilibrium value for $f_a \lesssim 10^{10}$ GeV so that $\Delta N_{\rm eff}$ does not exceed 10^{-3} even for smaller f_a. Therefore, we can conclude that the relativistic axion abundance is far below the current limit on dark radiation from PLANCK [32].

6.1.2 10^{12} GeV$\lesssim f_a \lesssim 10^{14}$ GeV

In this region, saxions and axinos do not dominate the universe, but they do decay after neutralino freeze-out. In addition, saxion production from coherent oscillation becomes

larger than thermal production as shown in Figs. 7*a*) and 8*a*). Such late decays of saxions and axinos can produce an overabundance of neutralino dark matter particles which then re-annihilate to deplete their initial density. To discuss the neutralino dark matter density in this region, let us consider the saxion decay temperature:

$$T_D^s \simeq 3.1\ \text{GeV} \times \xi \left(1 + \frac{2c_H^2\mu^2}{\xi^2 m_s^2}\right)^{1/2} \left(\frac{90}{g_*}\right)^{1/4} \left(\frac{m_s}{5\ \text{TeV}}\right)^{3/2} \left(\frac{10^{13}\ \text{GeV}}{f_a}\right). \tag{6.4}$$

Note that the standard neutralino freeze-out temperature $T_{\rm fr}$ is around 5 GeV. Thus, the saxion decay temperature gets smaller than $T_{\rm fr}$ when $f_a \gtrsim 10^{13}$ GeV for $\xi \sim 1$, or when $f_a \gtrsim 10^{12}$ GeV for $\xi \lesssim 0.1$. The axino decay temperature is

$$T_D^{\tilde{a}} \simeq 3.7\ \text{GeV} \times c_H \left(\frac{90}{g_*}\right)^{1/4} \left(\frac{\mu}{150\ \text{GeV}}\right) \left(\frac{10^{12}\ \text{GeV}}{f_a}\right) \left(\frac{m_{\tilde{a}}}{5\ \text{TeV}}\right)^{1/2}, \tag{6.5}$$

which can be smaller $T_{\rm fr}$ when $f_a \gtrsim 10^{12}$ GeV. The neutralino density determined from the re-annihilation process is given by

$$\begin{aligned} Y_{\widetilde{Z}_1}^{-1}(T < T_D) &\simeq Y_{\widetilde{Z}_1}^{-1}(T_D) + \left(Y_{\widetilde{Z}_1}^{\rm re-an}\right)^{-1} \\ &= Y_{\widetilde{Z}_1}^{-1}(T_D) + \frac{4\langle\sigma v\rangle M_p T_D}{\left(90/\pi^2 g_*(T_D)\right)^{1/2}} \end{aligned} \tag{6.6}$$

where $Y_{\widetilde{Z}_1}(T_D) = Y_{\widetilde{Z}_1}^{\rm fr} + Y_{\widetilde{Z}_1}^{\rm decay}$ and T_D can be either T_D^s or $T_D^{\tilde{a}}$. For 10^{12} GeV$\lesssim f_a \lesssim 10^{14}$ GeV, neutralino production due to axino/saxion decay is then much larger than that from the standard neutralino freeze-out, *i.e.* $Y_{\widetilde{Z}_1}(T_D) \simeq Y_{\widetilde{Z}_1}^{\rm decay}$. The neutralino abundance dominated by the re-annihilation term $Y_{\widetilde{Z}_1}^{\rm re-an}$ of Eq. (6.6) is approximated by

$$\begin{aligned} Y_{\widetilde{Z}_1}(T < T_D) \approx 4.1 \times 10^{-13} \frac{1}{c_H} \left(\frac{g_*}{90}\right)^{1/4} \left(\frac{2.57 \times 10^{-25}\ \text{cm}^3/\text{s}}{\langle\sigma v\rangle}\right) \\ \times \left(\frac{150\ \text{GeV}}{\mu}\right) \left(\frac{f_a}{10^{12}\ \text{GeV}}\right) \left(\frac{5\ \text{TeV}}{m_{\tilde{a}}}\right)^{1/2}. \end{aligned} \tag{6.7}$$

The schematic behavior of the neutralino yield from standard freeze-out, axino decay, saxion decay and re-annihilation is shown in Fig. 10.

One of the most important features is that the neutralino density can be larger than the standard density for $f_a \gtrsim 10^{12}$ GeV. This can cause a conflict with the direct detection bound from XENON100 since Higgsino-like WIMPs have a large spin-independent nucleon scattering cross-section. From the neutralino yield via re-annihilation, Eq. (6.7), we get the neutralino dark matter density

$$\begin{aligned} \Omega_{\widetilde{Z}_1} h^2 &\simeq \frac{m_{\widetilde{Z}_1} Y_{\widetilde{Z}_1}}{3.6\,\text{eV}} \\ &= 0.015 \times c_H \left(\frac{g_*}{90}\right)^{1/4} \left(\frac{2.57 \times 10^{-25}\ \text{cm}^3/\text{s}}{\langle\sigma v\rangle}\right) \\ &\quad \times \left(\frac{150\ \text{GeV}}{\mu}\right) \left(\frac{f_a}{10^{12}\ \text{GeV}}\right) \left(\frac{5\ \text{TeV}}{m_{\tilde{a}}}\right)^{1/2} \left(\frac{m_{\widetilde{Z}_1}}{135\ \text{GeV}}\right). \end{aligned} \tag{6.8}$$

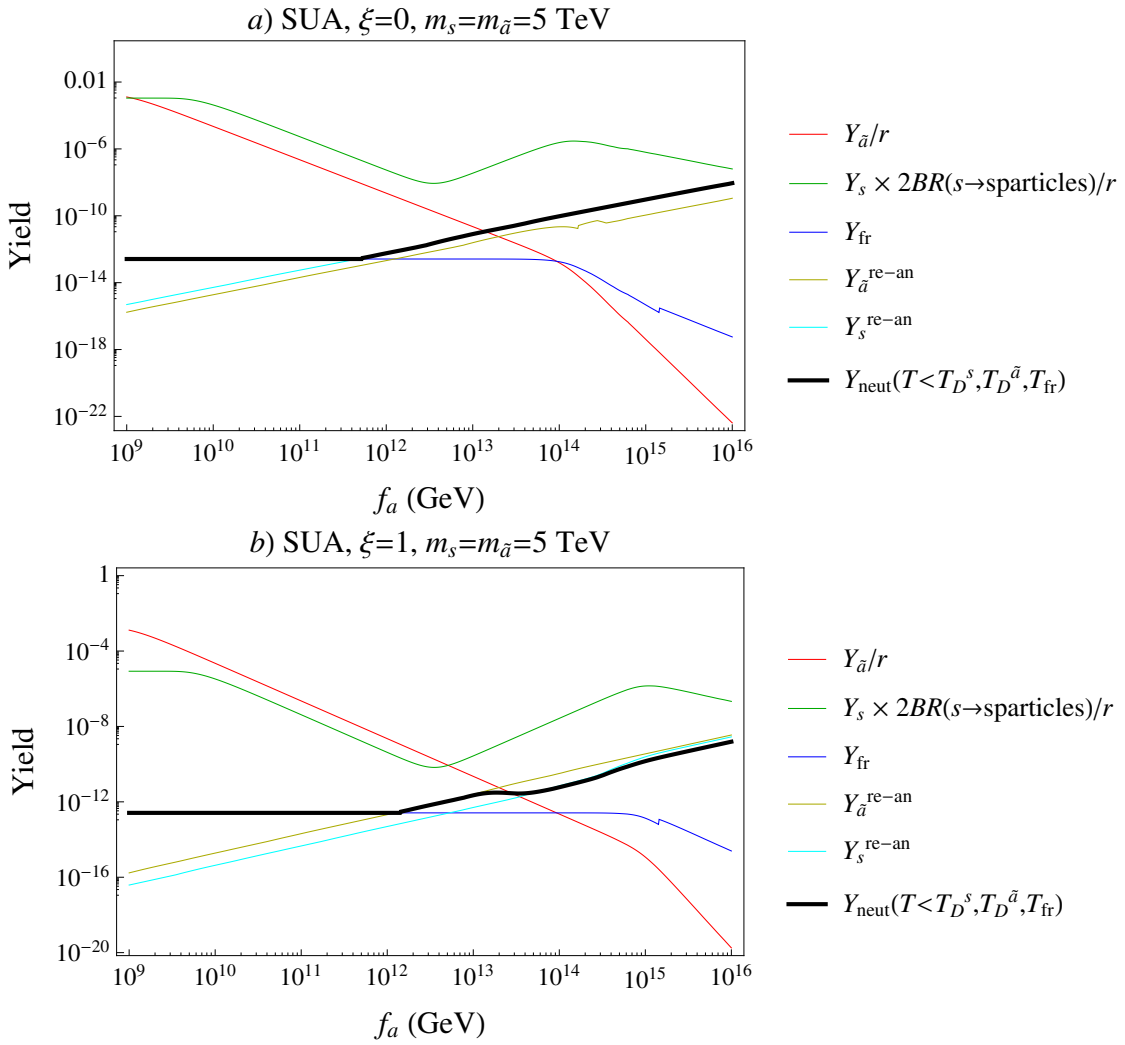

Figure 10: Neutralino yield from standard freeze-out and decay. We use *a)* $\xi = 0$ and *b)* $\xi = 1$. $Y_{\tilde{a}}^{\rm re-an}$ ($Y_s^{\rm re-an}$) is the re-annihilation contribution for neutralino density from axino (saxion) decay. $Y_{\rm neut}$ is the final neutralino yield.

This has to be compared with the neutralino density bound from the XENON100 experiment [33] for the SUA benchmark point which is

$$\Omega_{\tilde{Z}_1}^{Xe} h^2 < 0.026. \tag{6.9}$$

Therefore, we get the bound: $f_a/c_H \lesssim 2 \times 10^{12}$ GeV, which again requires the cold axion as a major component of dark matter. Of course, this constraint can be avoided for the case of a more purely Higgsino-like dark matter scenario (with larger bino/wino mass) to saturate the dark matter density ($\Omega_{\tilde{Z}_1} h^2 = 0.11$) by the re-annihilation process. That is, we can open the possibility for Higgsino-like dark matter which is more abundant than in the standard cosmology in this region of f_a.

Concerning the constraint from dark radiation, the situation is not much different from the case of $f \lesssim 10^{12}$ GeV. Although saxion and axino decay after neutralino freeze-out, there is no matter domination era in this region, and thus the produced axion abundance from saxion decay is described again by Eq. (6.3) which gives an even smaller amount of dark radiation for larger f_a.

6.1.3 $f_a \gtrsim 10^{14}$ GeV

Although thermally produced saxions and axinos do not dominate the universe at large f_a, oscillation production of saxions can dominate for large enough f_a as discussed in the previous section. We rewrite the condition for coherent oscillations of saxions to dominate the universe:

$$f_a \gtrsim 2.7 \times 10^{14}\ \text{GeV} \times \xi^{1/3} \left(1 + \frac{2c_H^2\mu^2}{\xi^2 m_s^2}\right)^{1/6} \left(\frac{10}{g_*}\right)^{1/12} \left(\frac{10^7\ \text{GeV}}{\min[T_R, T_s]}\right)^{1/3} \left(\frac{m_s}{5\text{TeV}}\right)^{1/2}. \tag{6.10}$$

In this region, cosmology becomes more interesting. As the saxion coherent oscillation dominates the universe, the neutralino dark matter density, radiation and dark radiation are all determined by branching ratios of the saxion decays into sparticles, SM particles and axions.

Under the sudden decay approximation, we can obtain the number of effective neutrinos [34]:

$$\begin{aligned} \Delta N_{\text{eff}} &= 18 \times \frac{3}{4} g_*(T_D^s)^{-1/3} \left[\frac{BR(s \to aa)}{1 - BR(s \to aa)}\right] \\ &\simeq 14 \times g_*(T_D^s)^{-1/3} \frac{\xi^2 m_s^2}{2c_H^2\mu^2} \\ &= 3.5 \times 10^3\ \frac{\xi^2}{c_H^2} \left(\frac{10}{g_*(T_D^s)}\right)^{1/3} \left(\frac{m_s}{5\ \text{TeV}}\right)^2 \left(\frac{150\ \text{GeV}}{\mu}\right)^2. \end{aligned} \tag{6.11}$$

Note that we assume that most of the neutralinos produced by saxion decay re-annihilate into SM particles which eventually contribute to radiation. The formula shows that the dark radiation constraint is very severe in this region of large f_a. This arises from the fact that saxion decay into axion pairs is the dominant mode for large m_s. If the saxion mass is around $\mu = 150$ GeV, it is possible to obtain $\Delta N_{\text{eff}} \lesssim 1$ (see an example in Fig. 11*c*). Otherwise, ξ should be suppressed to be $\mathcal{O}(0.01)$. Note that a smaller saxion mass makes the saxion decay temperature smaller down to $\mathcal{O}(1)$ MeV for $f_a \gtrsim 10^{14}$ GeV (see Eq. (6.14)) so that such a region is now constrained by BBN (see Fig. 11*a*).

In Fig. 9, we show the ΔN_{eff} for $m_s = 5$ TeV. As discussed before, ΔN_{eff} is well below the current limit for $f_a \lesssim 10^{14}$ GeV. For $f_a \gtrsim 10^{14}$ GeV, ΔN_{eff} become larger than the current limit of 1.6, so this parameter region of f_a becomes excluded. Let us note that a terminal value of ΔN_{eff} described by Eq. (6.11) is reached for $f_a \gtrsim 10^{15}$ GeV. This is due to the fact that *only part of saxion decay contributes to the radiation energy so that the entropy dilution takes place for rather larger value of f_a than that of saxion domination.* The saxion domination and entropy dilution will be discussed in the following paragraphs.

After the period of the saxion domination, its decay overproduces neutralinos and their relic density is again determined by re-annihilation,

$$Y_{\widetilde{Z}_1}^{-1} \simeq \left(Y_{\widetilde{Z}_1}^{\rm fr} + Y_{\widetilde{Z}_1}^{\rm decay}\right)^{-1} \times r + \frac{4\langle\sigma v\rangle M_p T_D^s}{\left(90/\pi^2 g_*(T_D^s)\right)^{1/2}}, \tag{6.12}$$

where r is the entropy dilution factor which is given by

$$r = \max\left[1, \frac{4}{3}\left[1 - BR(s \to aa)\right]\frac{Y_s m_s}{T_D^s}\right]. \tag{6.13}$$

The decay temperature of the saxion is determined by the visible energy density from the saxion decay and is given by [35]

$$\begin{aligned} T_D^s &= \left[\{1 - BR(s \to aa)\}\frac{90}{\pi^2 g_*}\right]^{1/4}\sqrt{\Gamma_s M_p} \\ &\simeq 0.11\ {\rm GeV}\sqrt{\xi c_H}\left(1 + \frac{2c_H^2\mu^2}{\xi^2 m_s^2}\right)^{1/4}\left(\frac{10}{g_*}\right)^{1/4} \\ &\quad \times \left(\frac{\mu}{150\ {\rm GeV}}\right)^{1/2}\left(\frac{m_s}{5\ {\rm TeV}}\right)\left(\frac{10^{14}\ {\rm GeV}}{f_a}\right). \end{aligned} \tag{6.14}$$

In this parameter region, neutralinos are produced mostly by saxion decay, and thus the first term of Eq. (6.12) is simply given by

$$\begin{aligned} Y_{\widetilde{Z}_1}^{\rm decay} &\simeq Y_s^{\rm CO} \times 2BR(s \to {\rm sparticles}) \\ &\simeq 6.8 \times 10^{-5}\ \frac{c_H^2}{\xi^2}\left(1 + \frac{2c_H^2\mu^2}{\xi^2 m_s^2}\right)^{-1}\left(\frac{\min[T_R, T_s]}{10^7\ {\rm GeV}}\right) \\ &\quad \times \left(\frac{f_a}{10^{14}\ {\rm GeV}}\right)^2\left(\frac{\mu}{150\ {\rm GeV}}\right)^2\left(\frac{5\ {\rm TeV}}{m_s}\right)^3 \end{aligned} \tag{6.15}$$

if there is no dilution, or

$$Y_{\widetilde{Z}_1}^{\rm decay} \times \frac{1}{r} \simeq \frac{3Y_s \times 2BR(s \to {\rm sparticles})T_D^s}{4\left[1 - BR(s \to aa)\right]Y_s m_s} \tag{6.16}$$

if the dilution factor r is larger than unity. For large enough m_s, we have $1 - BR(s \to aa) \simeq BR(s \to {\rm sparticles})$ leading to

$$\begin{aligned} Y_{\widetilde{Z}_1}^{\rm decay} \times \frac{1}{r} \simeq \frac{3T_D^s}{2m_s} &= 3.3 \times 10^{-5}\sqrt{\xi c_H}\left(1 + \frac{2c_H^2\mu^2}{\xi^2 m_s^2}\right)^{1/4}\left(\frac{10}{g_*}\right)^{1/4} \\ &\quad \times \left(\frac{\mu}{150\ {\rm GeV}}\right)^{1/2}\left(\frac{10^{14}\ {\rm GeV}}{f_a}\right). \end{aligned} \tag{6.17}$$

Now, the re-annihilation part becomes

$$\begin{aligned} Y_{\widetilde{Z}_1}^{\rm re-an} &\equiv \frac{\left(90/\pi^2 g_*(T_D^s)\right)^{1/2}}{4\langle\sigma v\rangle M_p T_D^s} \\ &\simeq 4.1 \times 10^{-11}\ \frac{1}{\sqrt{\xi c_H}}\left(\frac{10}{g_*}\right)^{1/4}\left(1 + \frac{2c_H^2\mu^2}{\xi^2 m_s^2}\right)^{-1/4}\left(\frac{2.57 \times 10^{-25}\ {\rm cm}^3/{\rm s}}{\langle\sigma v\rangle}\right) \\ &\quad \times \left(\frac{150\ {\rm GeV}}{\mu}\right)^{1/2}\left(\frac{f_a}{10^{14}\ {\rm GeV}}\right)\left(\frac{5\ {\rm TeV}}{m_s}\right). \end{aligned} \tag{6.18}$$

Comparing $Y_{\widetilde{Z}_1}^{\rm decay}/r$ and $Y_{\widetilde{Z}_1}^{\rm re-an}$, we find that the re-annihilation dominantly determines the neutralino density for $f_a \lesssim 10^{17}$ GeV. Therefore, the abundance of neutralinos is

$$\begin{aligned}\Omega_{\widetilde{Z}_1}h^2 &= \left(\frac{m_{\widetilde{Z}_1}Y_{\widetilde{Z}_1}}{3.6\,\mathrm{eV}}\right)\\ &\simeq 1.5\,\frac{1}{\sqrt{\xi c_H}}\left(\frac{10}{g_*}\right)^{1/4}\left(1+\frac{2c_H^2\mu^2}{\xi^2 m_s^2}\right)^{-1/4}\left(\frac{2.57\times10^{-25}\ \mathrm{cm}^3/\mathrm{s}}{\langle\sigma v\rangle}\right)\\ &\quad\times\left(\frac{150\ \mathrm{GeV}}{\mu}\right)^{1/2}\left(\frac{f_a}{10^{14}\ \mathrm{GeV}}\right)\left(\frac{5\ \mathrm{TeV}}{m_s}\right)\left(\frac{m_{\widetilde{Z}_1}}{135\,\mathrm{GeV}}\right). \end{aligned} \tag{6.19}$$

The schematic plots for neutralino yield are shown in Fig. 10. The neutralino abundance is much larger than the observed value for $f_a = 10^{14}$ GeV. This provides a serious constraint for the model together with $\Delta N_{\rm eff}$.

To avoid the problem of overclosure density of neutralinos, we may consider a case with a light enough saxion such that decay to neutralinos is forbidden; then saxion decay produces only axion pairs and entropy. The various temperatures, yields and ΔN_{eff} are shown in frames *a*), *b*) and *c*) of Fig. 11. In this case, the existing relic particles are diluted away as shown in frame *b*). Even in this case, however, BBN strongly constrains the large f_a region as discussed previously.

6.2 SOA

Similarly to the SUA case, we divide the region of f_a into three parts: $f_a \lesssim 10^{13}$ GeV, 10^{13} GeV$\lesssim f_a \lesssim 10^{14}$ and $f_a \gtrsim 10^{14}$ GeV, which correspond to the regions of the saxion/axino decay before the neutralino freeze-out, after the freeze-out, and the saxion domination before its decay, respectively. One crucial difference arises due to the fact that μ is very large for SOA compared to the SUA case. Such a large μ makes the saxion decay temperature (for $m_s \lesssim 5$ TeV) one or two orders of magnitude larger than the SUA case as shown in Figs. 3*a*) and 4*b*). As discussed in the SUA case, large f_a might cause overproduction of neutralinos and relativistic axions from the saxion decay. Such problems can be avoided by considering a light saxion that does not decay into sparticle pairs, and a small ξ to suppress $BR(s \to aa)$. However, the conflict with BBN coming from the saxion decay temperature close to $\mathcal{O}(1)$ MeV is hardly circumvented as shown in Eq. (6.14). In the SOA case, this tension is relieved as the saxion decay temperature is enhanced by large μ even for lighter saxion masses. Thus, we will take a smaller saxion mass to discuss cosmological implications for the SOA benchmark point.

6.2.1 $f_a \lesssim 10^{13}$ GeV

This region is basically ruled out by overproduction of the neutralino dark matter: since saxions and axinos decay before neutralino freeze-out (see Figs. 7*b*) and 8*b*)), the standard relic overabundance is unaltered: $\Omega_{\widetilde{Z}_1}h^2 = 6.8$.

For the effective number of neutrinos, we can rewrite Eq. (6.3) inserting the SOA benchmark parameters:

$$\Delta N_{\rm eff} \approx 1.6\times10^{-10}\,\frac{\xi^2\zeta_s}{c_H}\left(1+\frac{\xi^2 m_s^4}{16c_H^2\mu^4}\right)^{-3/2}\left(\frac{g_{*s}}{90}\right)^{-1/3}\left(\frac{g_*}{90}\right)^{1/4}$$

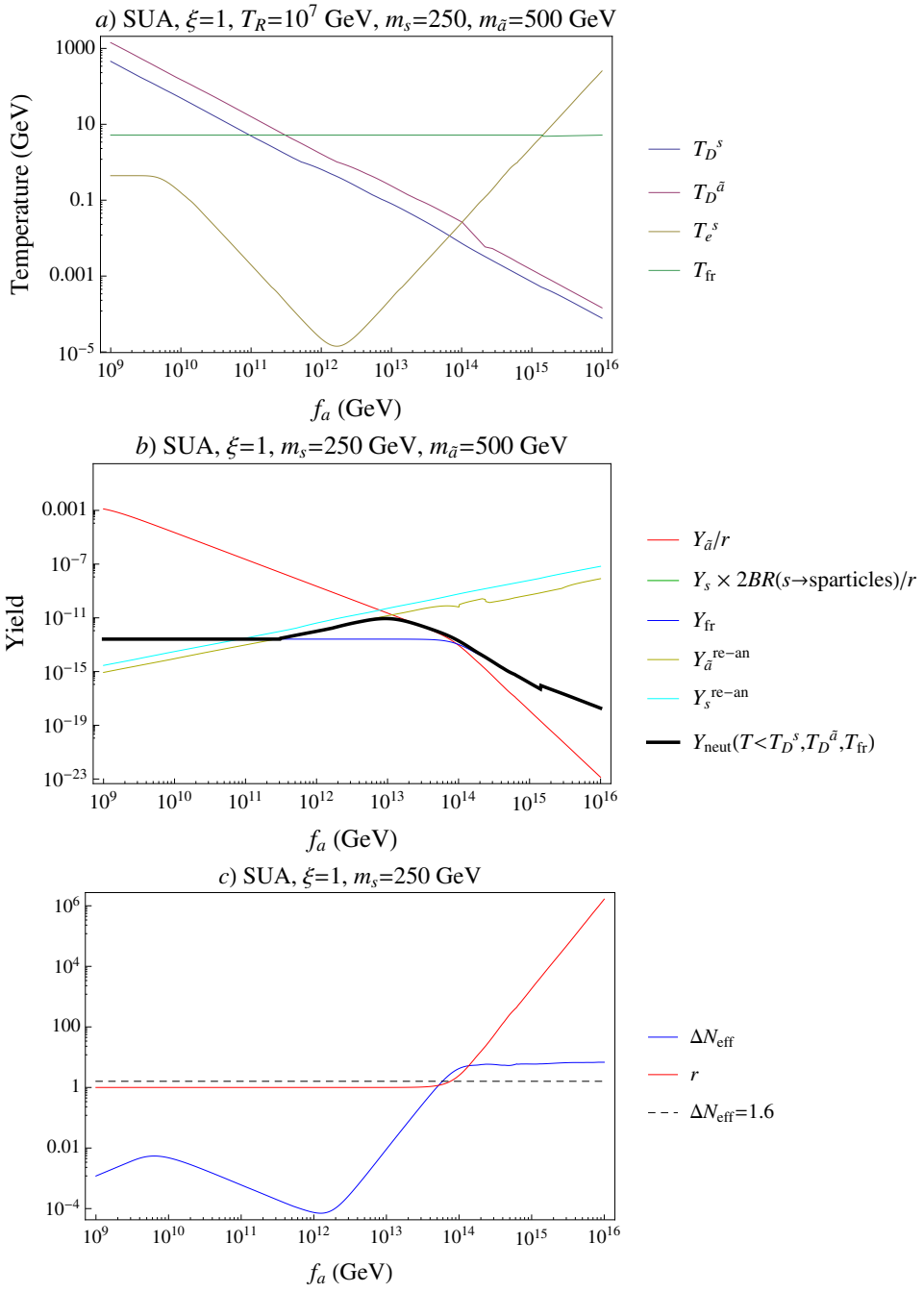

Figure 11: Plots for the SUA case with $\xi = 1$, $T_R = 10^7$ GeV and $m_s = 250$ GeV. *a*) Saxion decay temperature (blue), saxion-radiation equality temperature (red) and neutralino freeze-out temperature in the standard cosmology (yellow) are shown. *b*) Neutralino yield from standard freeze-out and decay. *c*) $\Delta N_{\rm eff}$ and r.

$$\times \left(\frac{2.6\ \text{TeV}}{\mu}\right)^6 \left(\frac{B\mu/\mu \text{ or } \mu}{\text{TeV}}\right)^2 \left(\frac{10^{12}\ \text{GeV}}{f_a}\right) \left(\frac{m_s}{500\ \text{GeV}}\right)^{11/2}. \qquad (6.20)$$

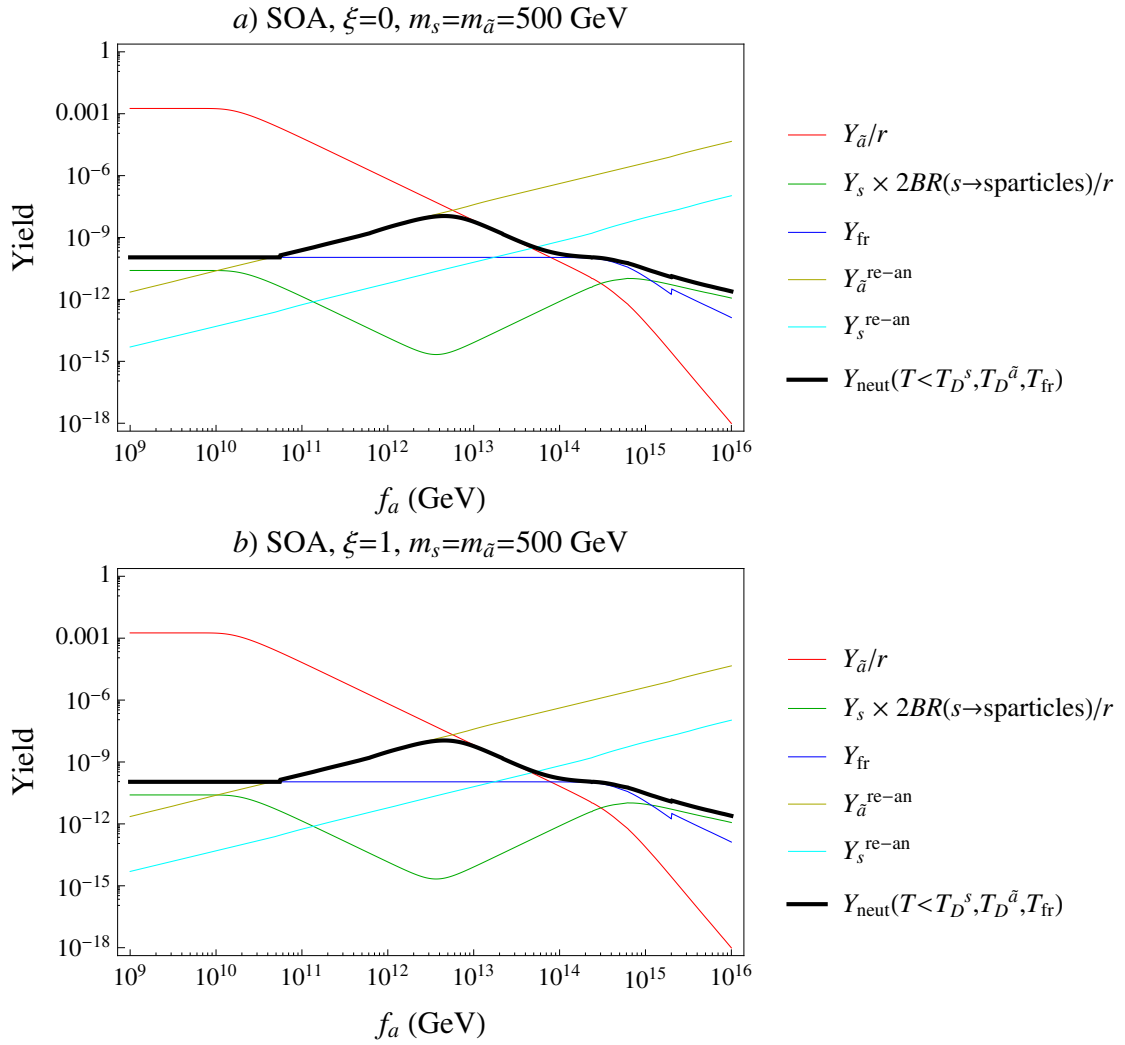

Figure 12: Neutralino yield from standard freeze-out and decay. We use *a)* $\xi = 0$ and *b)* $\xi = 1$.

Here we used the fact that the only relevant decay modes of the saxion are $s \to hh$, W^+W^-, ZZ and aa, which leads to the approximate expressions of T_D^s and $BR(s \to aa)$ for $m_s \sim 500$ GeV as follows:

$$T_D^s \approx \left(\frac{c_H^2\mu^4}{4\pi v_{PQ}^2 m_s}\right)^{1/2} \left(1 + \frac{\xi^2 m_s^4}{16 c_H^2 \mu^4}\right)^{1/2} M_p^{1/2} \left(\frac{90}{\pi^2 g_*}\right)^{1/4}, \tag{6.21}$$

$$BR(s \to aa) \approx \frac{\xi^2 m_s^4}{16 c_H^2 \mu^4} \left(1 + \frac{\xi^2 m_s^4}{16 c_H^2 \mu^4}\right)^{-1}. \tag{6.22}$$

Again $\Delta N_{\rm eff}$ is negligibly small (see Fig. 13).

6.2.2 10^{13} GeV$\lesssim f_a \lesssim 10^{14}$ GeV

In this region, saxions and axinos decay after the neutralino freeze-out but still decay

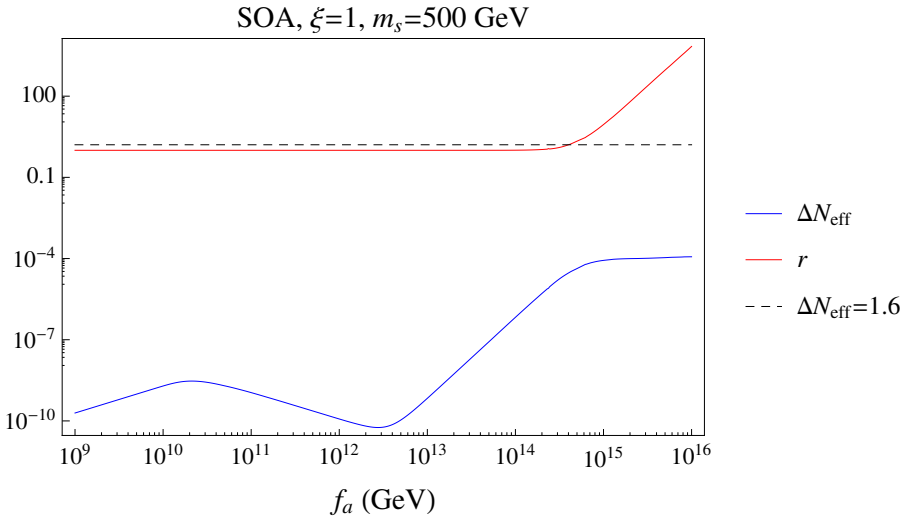

Figure 13: Plot for $\Delta N_{\rm eff}$ and r in SOA, $\xi = 1$ and $m_s = 500$ GeV.

before matter domination can take place. The neutralino density can thus be augmented by saxion or axino decay while there is no entropy dilution. Therefore, this region is also excluded by dark matter overproduction.

6.2.3 $f_a \gtrsim 10^{14}$ GeV

In this region, the saxion coherent oscillation can dominate the universe and thus the saxion decays into SM particles, sparticles and axions determine the important cosmological quantities, *i.e.*, the amounts of entropy dilution, neutralino density and dark radiation.

As in the SUA case (with $r > 1$), the number of effective neutrinos is determined by

$$\begin{aligned}\Delta N_{\rm eff} &\simeq 14 \times g_*(T_D^s)^{-1/3} \frac{\xi^2 m_s^4}{16 c_H^2 \mu^4} \\ &= 5.6 \times 10^{-4}\ \frac{\xi^2}{c_H^2} \left(\frac{10}{g_*(T_D^s)}\right)^{1/3} \left(\frac{m_s}{500\ \text{GeV}}\right)^4 \left(\frac{2.6\ \text{TeV}}{\mu}\right)^4 . \end{aligned} \tag{6.23}$$

Thus, $\Delta N_{\rm eff}$ is negligible for the case of the SOA parameters.

The most important feature resides in the neutralino density. The neutralino production from the saxion and axino decay is not very large as shown in Fig. 12, but there is a huge amount of entropy produced since the saxion dominantly decays into Higgs and gauge boson states as can be seen in Figs. 1*b*) and 2*b*). The dilution factor r is given by

$$\begin{aligned} r = \frac{T_e^s}{T_D^s} &\approx 24 \times c_H^{-1} \left(\frac{90}{g_*}\right)^{-1/4} \left(1 + \frac{\xi^2 m_s^4}{16 c_H^2 \mu^4}\right)^{-1/2} \\ &\times \left(\frac{2.6\ \text{TeV}}{\mu}\right)^2 \left(\frac{\min[T_R, T_s]}{10^7\ \text{GeV}}\right) \left(\frac{f_a}{10^{15}\ \text{GeV}}\right)^3 \left(\frac{m_s}{500\ \text{GeV}}\right)^{1/2} . \end{aligned} \tag{6.24}$$

Here we used the saxion decay temperature given by

$$T_D^s \approx 0.11 \text{ GeV} \times c_H \left(\frac{90}{g_*}\right)^{1/4} \left(1+\frac{\xi^2 m_s^4}{16 c_H^2 \mu^4}\right)^{1/2} \times \left(\frac{\mu}{2.6 \text{ TeV}}\right)^2 \left(\frac{10^{15} \text{ GeV}}{f_a}\right) \left(\frac{500 \text{ GeV}}{m_s}\right)^{1/2}, \tag{6.25}$$

and radiation-saxion equality temperature,

$$T_e^s = \frac{4}{3} m_s Y_s^{\text{CO}} = 2.5 \text{ GeV} \left(\frac{\min[T_R, T_s]}{10^7 \text{ GeV}}\right) \left(\frac{f_a}{10^{15} \text{ GeV}}\right)^2. \tag{6.26}$$

Notice that r can be as large as $\mathcal{O}(1000)$ for $f_a \sim 10^{16}$ GeV as shown in Fig. 13. Therefore, the neutralino density can be $\mathcal{O}(1/1000)$ times smaller than the standard density as shown in Fig. 12 and so the overproduction constraint can be avoided. The saxion decay temperature is around 10 MeV even for $f_a \sim 10^{16}$ GeV leaving unchanged the standard BBN prediction.

7. Conclusion

The supersymmetric DFSZ axion model is highly motivated in that it provides 1. the SUSY solution to the gauge hierarchy problem, 2. the Peccei-Quinn-Weinberg-Wilczek solution to the strong CP problem and 3. the Kim-Nilles solution to the SUSY μ problem. We examined production rates for mixed axion/neutralino dark matter within the SUSY DFSZ model for a standard underabundance model (SUA) and a standard overabundance model (SOA). Much of the cosmology depends on the axino and saxion decay modes which are very different than those expected from the SUSY KSVZ model. In SUSY DFSZ, the direct coupling of axinos and saxions to the Higgs supermultiplets allows for rapid decays into various Higgs-Higgs, Higgs-Higgsino and diboson final states which do not occur in the SUSY KSVZ model.

For the SUA case (which has low $\mu \sim 150$ GeV as required by naturalness), the dark matter scenarios broke up into three main cases. For the lower range of $f_a \lesssim 10^{12}$ GeV, axinos and saxions can be thermally produced, but decay before the neutralino freeze-out, so that the standard relic neutralino abundance holds true. In this case of underabundant neutralinos, the remaining dark matter is composed of axions. For SUA, Higgsino-like WIMPs comprise $\sim 10\%$ of the CDM while axions comprise $\sim 90\%$. Dark radiation from $s \to aa$ decay is scant. For $f_a \sim 10^{12} - 10^{14}$ GeV, saxions and axinos do not dominate the universe, but do decay after the neutralino freeze-out, augmenting the standard abundance. The remaining axion abundance can always be adjusted using the initial misalignment θ_i so that the total mixed axion/neutralino abundance saturates $\Omega_{a\widetilde{Z}_1} h^2 \sim 0.12$ as long as neutralinos are not overproduced. For $f_a \gtrsim 10^{14}$ GeV, oscillation-produced saxions may dominate the universe and can overproduce both neutralino dark matter and dark radiation. However, in cases where m_s is light enough to forbid saxion decays to SUSY particles, and where ξ is small enough to suppress dark radiation, saxion decay to SM particles can lead

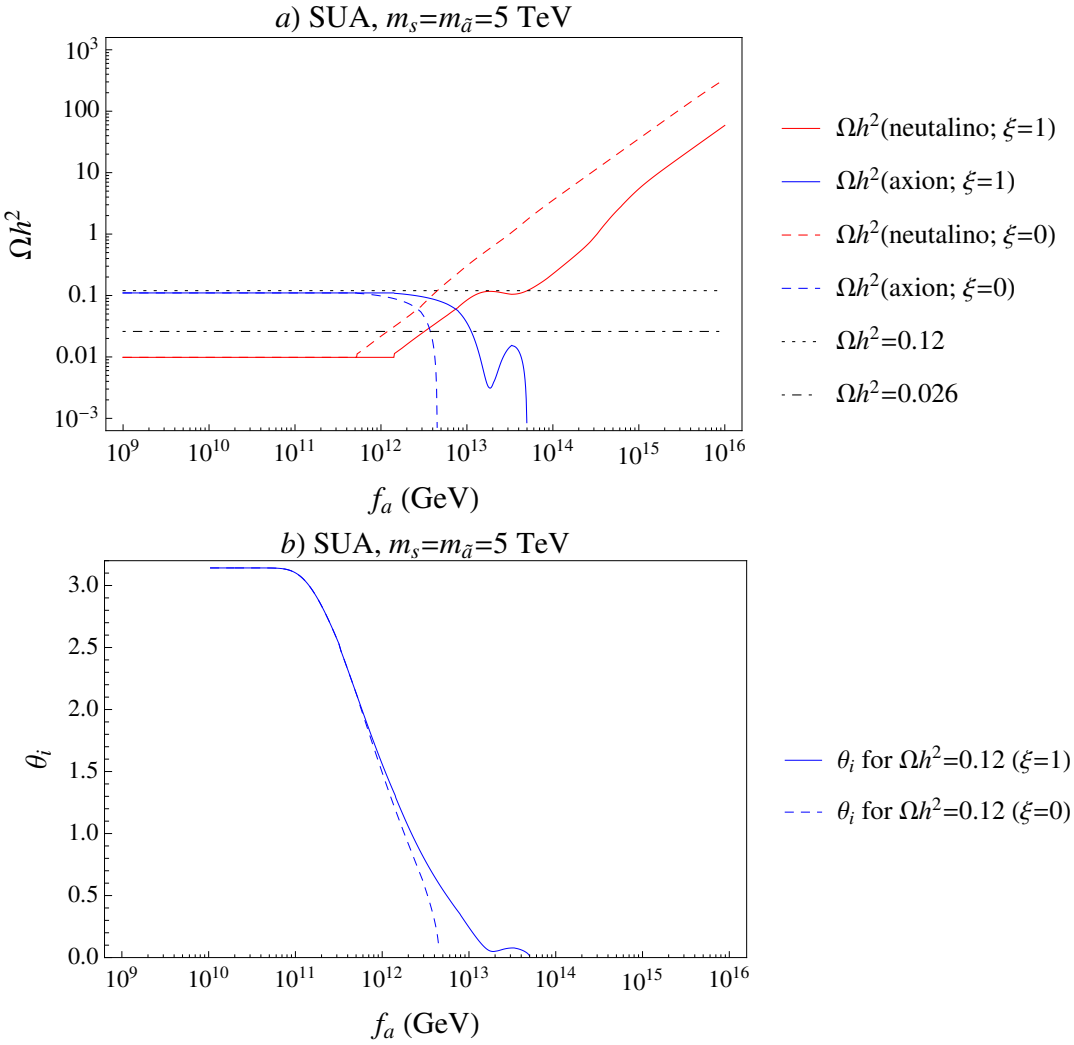

Figure 14: Plot of *a*) $\Omega_{\widetilde{Z}_1}h^2$ and $\Omega_a h^2$ vs. f_a for the SUA benchmark with $m_s = m_{\tilde{a}} = 5$ TeV for $\xi = 0$ (dashed) and $\xi = 1$ (solid). In *b*), we show the required axion misalignment angle θ_i required to saturate the mixed axion/neutralino abundance to match the measured value.

to large entropy dilution of neutralinos and axions so that the measured CDM abundance can be obtained.

Our summary plots for the SUA case are given in Figs. 14, 15 and 16 where the panels *a*) show the values of $\Omega_{\widetilde{Z}_1}h^2$ and $\Omega_a h^2$ versus f_a for $m_s = m_{\tilde{a}} = 5$ TeV, 10 TeV and 20 TeV, respectively. Dashed curves are for $\xi = 0$ while solid curves are for $\xi = 1$. In panels *b*), we show the required value of the axion misalignment angle θ_i with which the total neutralino plus axion abundance saturates the measured value. From Fig. 14*a*), we see– over the large range of $f_a \sim 10^9 - 10^{12}$ GeV– that Higgsino-like WIMPs comprise just $\sim 10\%$ of the total dark matter abundance, while the remaining 90% is comprised of axions. This region of mainly axion CDM from natural SUSY models has been emphasized in Ref. [26].

For SUA, the spin-independent (SI) neutralino-proton scattering cross section is $\sigma^{\rm SI}(\widetilde{Z}_1 p) \simeq$

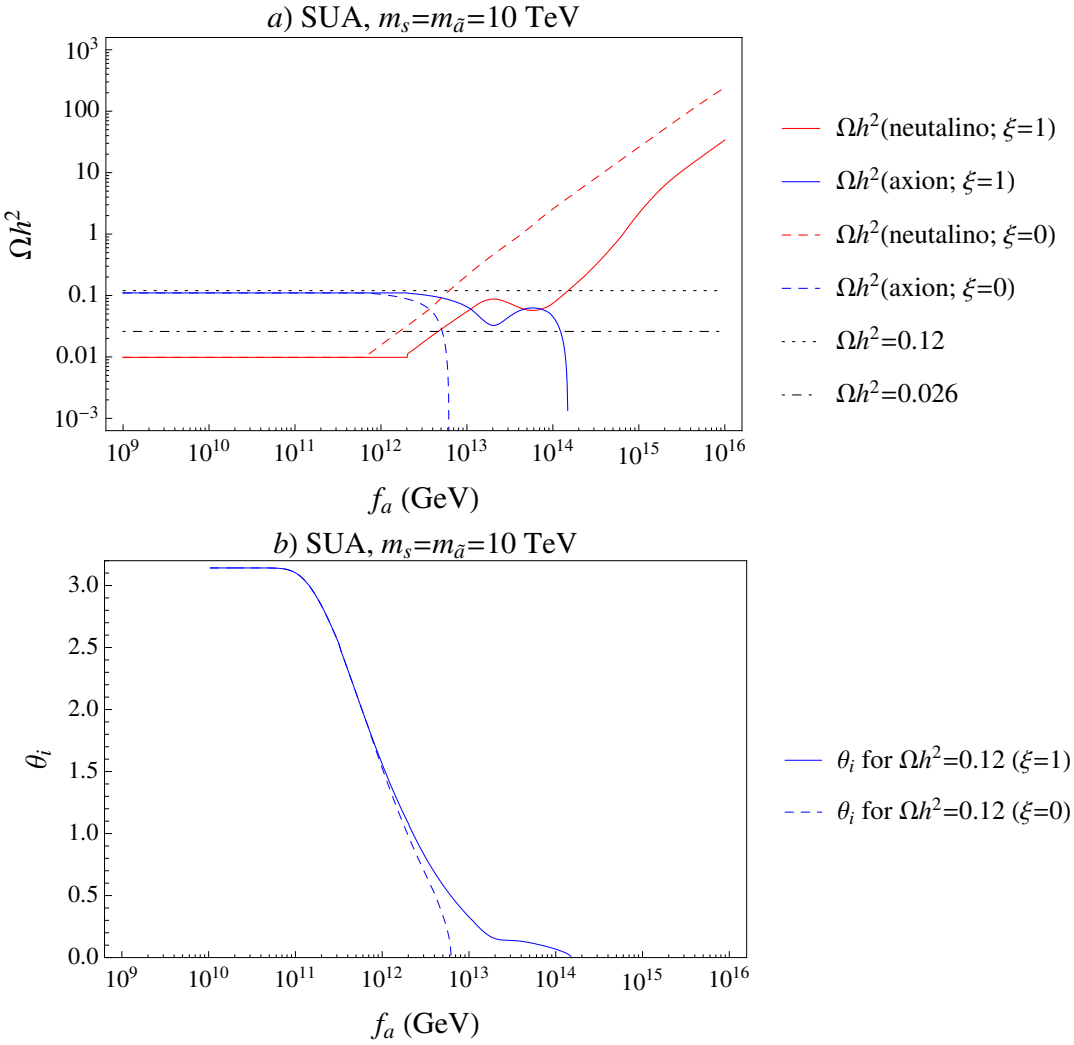

Figure 15: Plot of *a*) $\Omega_{\widetilde{Z}_1}h^2$ and $\Omega_a h^2$ vs. f_a for the SUA benchmark with $m_s = m_{\tilde{a}} = 10$ TeV for $\xi = 0$ (dashed) and $\xi = 1$ (solid). In *b*), we show the required axion misalignment angle θ_i required to saturate the mixed axion/neutralino abundance to match the measured value.

1.7×10^{-8} pb as shown in Table 1, whilst the limit from 225 live days of Xe-100 data taking [33] is $\sigma^{\rm SI}(\widetilde{Z}_1 p) \lesssim 4 \times 10^{-9}$ pb for a 135 GeV WIMP. This apparent conflict is easily reconciled within the SUA benchmark as the relic Higgsino-like WIMPs comprise only a fraction of the local relic density, and so the Xe-100 limits have to be rescaled downward by a factor $\Omega_{\widetilde{Z}_1}h^2/0.12$. For SUA with $f_a \lesssim 10^{12}$ GeV, the rescaling factor is ~ 0.1. The rescaled SI Higgsino-like WIMP detection rates compared against limits have been shown in Ref. [36] for a variety of radiatively-driven natural SUSY models. In Figs. 14, 15 and 16, also shown are the lines for $\Omega_{\widetilde{Z}_1}h^2 = 0.026$ below which the Xe-100 bound is evaded.

For the $\xi = 0$ case of Fig. 14*a*), the $\Omega_{\widetilde{Z}_1}h^2$ curve rises steadily with large $f_a \gtrsim 10^{12}$ GeV due to increasing production of saxions from coherent oscillations and their dominant decays to SUSY particles. This leads to subsequent neutralino re-annihilation at decreasing

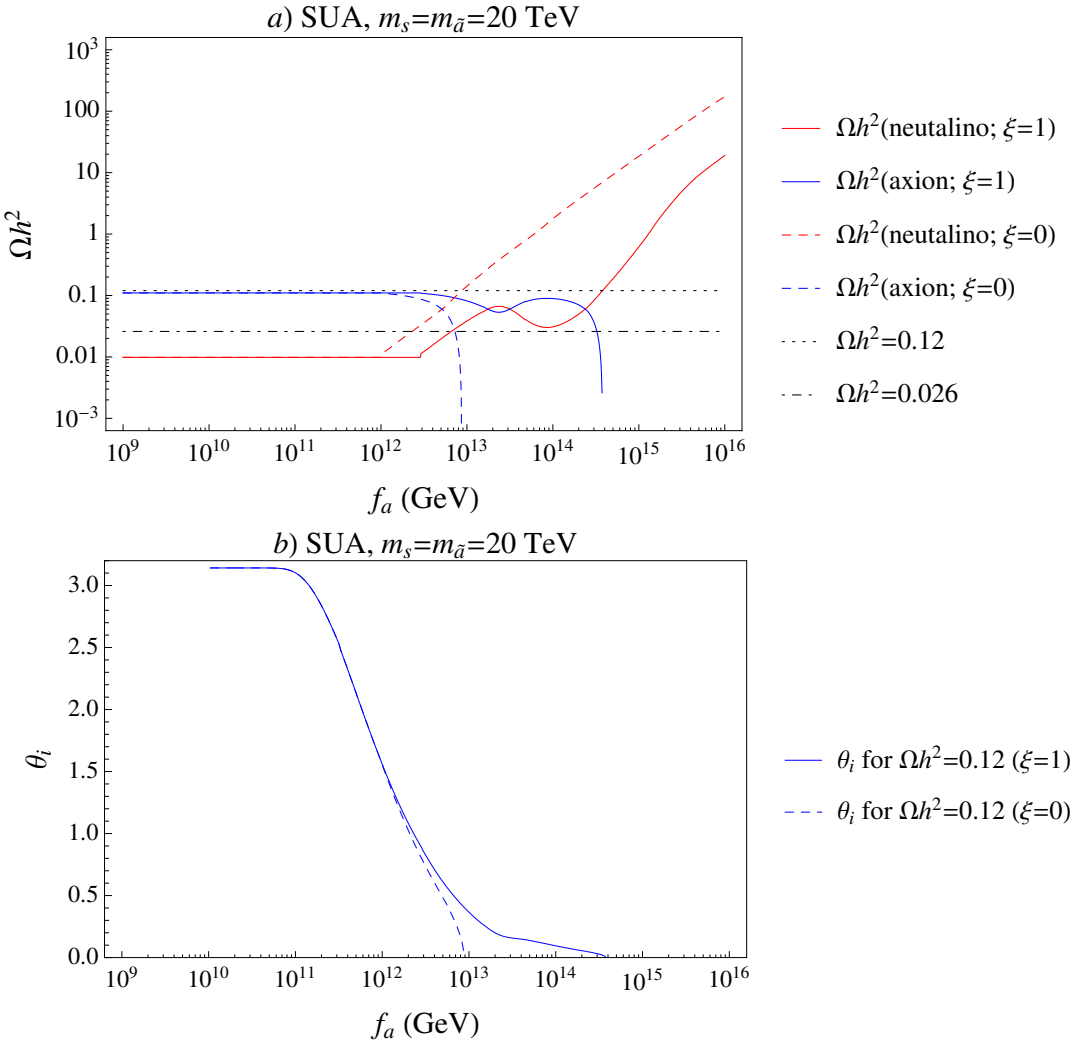

Figure 16: Plot of *a*) $\Omega_{\widetilde{Z}_1}h^2$ and $\Omega_a h^2$ vs. f_a for the SUA benchmark with $m_s = m_{\tilde{a}} = 20$ TeV for $\xi = 0$ (dashed) and $\xi = 1$ (solid). In *b*), we show the required axion misalignment angle θ_i required to saturate the mixed axion/neutralino abundance to match the measured value.

temperatures T_D^s. For $\xi = 1$, the dominant saxion decay mode is $s \to aa$, and decay-produced neutralinos come mainly from thermal axino production which decreases as f_a increases. One sees that $\Omega_{\widetilde{Z}_1}h^2$ turns over and briefly reaches $\Omega_{\widetilde{Z}_1}h^2 \simeq 0.12$ at $f_a \sim 3\times 10^{13}$ GeV before beginning again a rise due to increasing non-thermal saxion production. It is important to note that for $\xi \sim 1$ and $f_a \gtrsim 10^{14}$ GeV, too much dark radiation is produced ($\Delta N_{eff} > 1.6$, see Fig. 9) and thus very large f_a is excluded by overproduction of both dark radiation and WIMPs.

In all cases shown, axino and saxion decay widths become suppressed and they decay after neutralino freeze-out leading to an augmented neutralino abundance as f_a increases beyond 10^{12} GeV. In this region, WIMP dark matter becomes overproduced and the model becomes excluded. The excluded region occurs at higher f_a for $\xi = 1$ models since these

cases allow for $s \to aa$ decay which tends to be the dominant saxion decay mode when it is fully allowed; in such cases, the f_a value at which T_D drops below T_{fr} increases.

The axion misalignment angle shown in panels *b*) is required to be nearly $\theta_i \sim \pi$ for low $f_a \lesssim 10^{10}$ GeV but more natural values of θ_i occur for $f_a \sim 10^{10} - 10^{12}$ GeV. As $m_{\tilde{a}} = m_s$ is increased to 10 (20) TeV, the upper bound on f_a moves to 3×10^{12} (4×10^{12}) GeV for $\xi = 0$ as shown in Figs. 15 and 16. In the case of $\xi = 1$, there is a window of $\Omega_{\widetilde{Z}_1} h^2 < 0.12$ in the region of 10^{13} GeV$\lesssim f_a \lesssim 10^{14}$ GeV for $m_{\tilde{a}} = m_s \sim 10 - 20$ TeV. But, it is still above the Xe-100 limit, *i.e.* $\Omega_{\widetilde{Z}_1} h^2 > 0.026$, and thus this region is excluded within the SUA benchmark scenario.

For the SOA case with low $f_a \lesssim 10^{13}$ GeV, the standard neutralino abundance remains unchanged, and thus the model is excluded by the overabundance. As f_a is raised to 10^{14} GeV, saxions and axinos decay after the freeze-out, augmenting the neutralino overabundance even further. For $f_a \gtrsim 10^{14}$ GeV, as in the SUA case, the universe is dominated by oscillation-produced saxions leading to injection of even more neutralino dark matter as well as dark radiation. Thus, a large range of f_a is excluded in SOA by overproduction of dark matter, and also possibly by overproduction of dark radiation. An exception occurs for small m_s and low ξ where saxion decays to SUSY particles and axions are suppressed, and large entropy injection can bring the combined neutralino and axion abundance into accord with measured values. This is the case for $f_a \sim 5 \times 10^{15}$ GeV shown in Fig. 17 where $m_s = m_{\tilde{a}} = 0.5$ TeV is selected to close most of the lucrative saxion decay modes to SUSY particles. The axion abundance is suppressed appropriately by both entropy dilution and a small value of θ_i as shown in panel *b*).

Summary: We have considered R-parity conserving SUSY models with a standard under- and over-abundance of dark matter which invoke the PQWW solution to the strong CP problem via the SUSY DFSZ model, wherein Higgs superfields carry PQ charge, and which also provides a solution to the SUSY μ problem. For standard underabundant models, over a large range of PQ scale $f_a \sim 10^9 - 10^{12}$ GeV, saxions and axinos typically decay before neutralino freeze-out so that the WIMP portion of dark matter is expected to lie at its standard predicted value from thermal freeze-out, while axions would comprise the remainder. The relic neutralinos stand a good chance to be detectable at next generation WIMP direct detection experiments even with a depleted local abundance. Prospects for WIMP indirect detection should be more limited since expected rates go as the depleted abundance squared [36]. Prospects for microwave cavity detection of axions are good for the range of f_a where mainly axion dark matter is expected; in such cases, axions should be accessible to experimental searches [37]. For standard overabundant models, on the other hand, overabundant neutralino dark matter density can be appropriately depleted by a large entropy production from the oscillation-produced saxion decay. In this case, prospects for detecting both WIMP and axion dark matter are not promising.

Acknowledgments

We thank A. Lessa for ongoing collaboration on these topics.

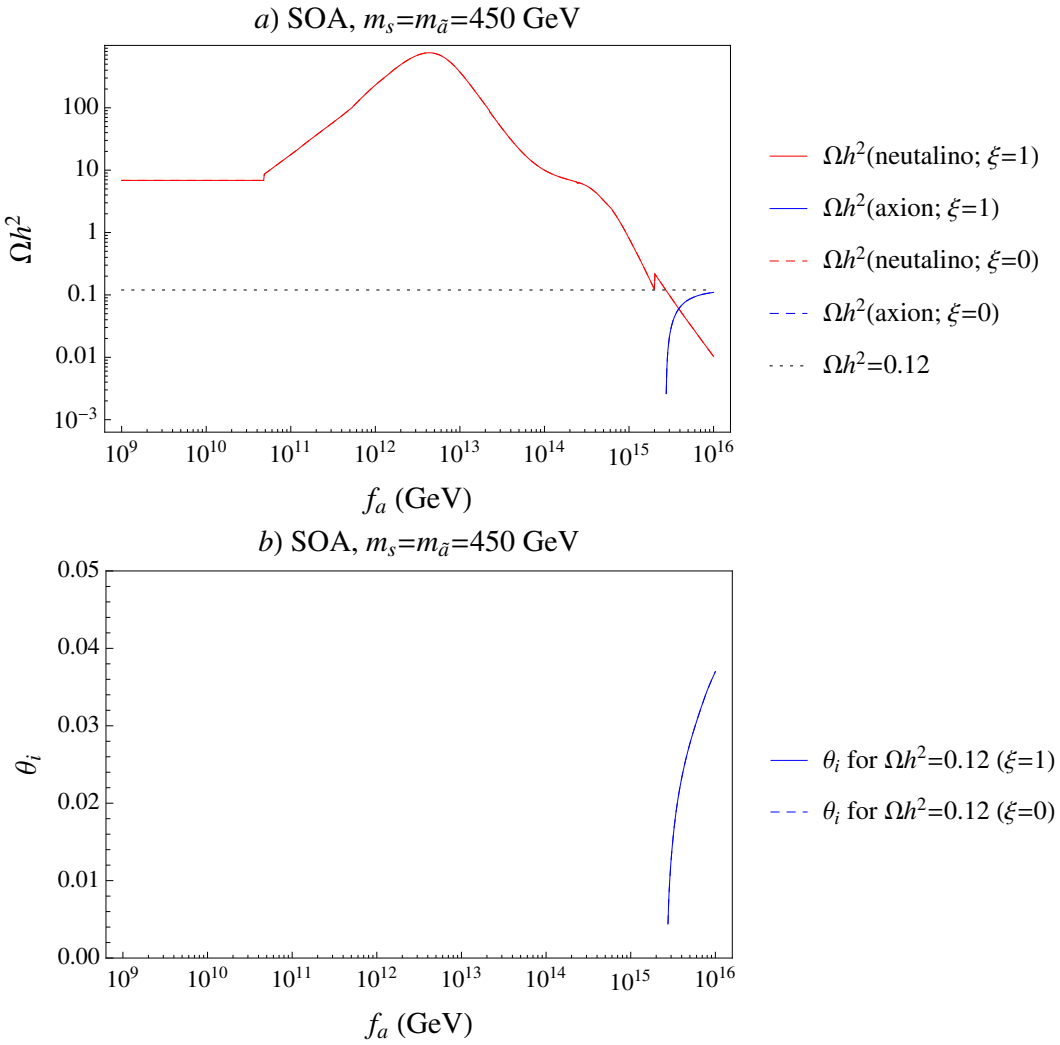

Figure 17: Plot of *a*) $\Omega_{\widetilde{Z}_1}h^2$ and $\Omega_a h^2$ vs. f_a for the SOA benchmark with $m_s = m_{\tilde{a}} = 0.5$ TeV for $\xi = 0$ (dashed) and $\xi = 1$ (solid). In *b*), we show the required axion misalignment angle θ_i required to saturate the mixed axion/neutralino abundance to match the measured value. Plots of $\xi = 1, 0$ cases are overlapped since $BR(s \to aa)$ is very tiny for small m_s region.

A. Appendix: partial decay widths of saxion and axino

We show the exact partial decay widths of saxion and axino at the tree-level. All the conventions are as in Ref. [38].

- $s \to \phi_i \phi_j$

$$\Gamma(s \to \phi_i \phi_j) = \frac{\lambda^2_{s\phi_i\phi_j}}{16\pi m_s}\lambda^{1/2}\left(1, \frac{m^2_{\phi_i}}{m^2_s}, \frac{m^2_{\phi_j}}{m^2_s}\right)\left(1 - \frac{1}{2}\delta_{ij}\right), \tag{A.1}$$

where $\phi_i = h, H, A, H^+, H^-$. Trilinear couplings are given by

$$\begin{aligned}
\lambda_{shh} &= \left(\frac{\sqrt{2}c_H\mu^2}{v_{PQ}}\right)\left\{1-\frac{1}{4}\left(\frac{m_A^2}{\mu^2}\right)\sin 2\beta\sin 2\alpha\right\} \\
&+\left(\frac{M_Z^2}{\sqrt{2}v}\right)\cos 2\alpha\sin(\beta-\alpha)\left[3\epsilon_h-\epsilon_H\left\{2\tan 2\alpha+\cot(\beta-\alpha)\right\}\right], \quad \text{(A.2)} \\
\lambda_{sHH} &= \left(\frac{\sqrt{2}c_H\mu^2}{v_{PQ}}\right)\left\{1+\frac{1}{4}\left(\frac{m_A^2}{\mu^2}\right)\sin 2\beta\sin 2\alpha\right\} \\
&+\left(\frac{M_Z^2}{\sqrt{2}v}\right)\cos 2\alpha\sin(\beta-\alpha)\left[3\epsilon_H\cot(\beta-\alpha)\right. \\
&\left.+\epsilon_h\left\{2\tan 2\alpha\cot(\beta-\alpha)-1\right\}\right], \quad \text{(A.3)} \\
\lambda_{shH} &= -\left(\frac{c_H m_A^2}{2\sqrt{2}v_{PQ}}\right)\sin 2\beta\cos 2\alpha \\
&+\left(\frac{M_Z^2}{\sqrt{2}v}\right)\cos 2\alpha\sin(\beta-\alpha)\left[-\epsilon_h\left\{2\tan 2\alpha+\cot(\beta-\alpha)\right\}\right. \\
&\left.+\epsilon_H\left\{2\tan 2\alpha\cot(\beta-\alpha)-1\right\}\right], \quad \text{(A.4)} \\
\lambda_{sAA} &= \left(\frac{\sqrt{2}c_H\mu^2}{v_{PQ}}\right)\left\{1+\frac{1}{4}\left(\frac{m_A^2}{\mu^2}\right)\sin^2 2\beta\right\} \\
&+\left(\frac{M_Z^2}{\sqrt{2}v}\right)\cos 2\beta\sin(\beta-\alpha)\left\{\epsilon_h-\epsilon_H\cot(\beta-\alpha)\right\}, \quad \text{(A.5)} \\
\lambda_{sH^+H^-} &= \left(\frac{\sqrt{2}c_H\mu^2}{v_{PQ}}\right)\left\{1+\frac{1}{4}\left(\frac{m_A^2}{\mu^2}\right)\sin^2 2\beta\right\} \\
&+\left(\frac{M_Z^2}{\sqrt{2}v}\right)\left[\cos 2\beta\sin(\beta-\alpha)\left\{\epsilon_h-\epsilon_H\cot(\beta-\alpha)\right\}\right. \\
&\left.+2\cos^2\theta_W\sin(\beta+\alpha)\left\{\epsilon_h+\epsilon_H\cot(\beta+\alpha)\right\}\right]. \quad \text{(A.6)}
\end{aligned}$$

- $s \to VV$

$$\begin{aligned}
\Gamma(s\to VV) &= \frac{g_V^2 g_{sVV}^2}{16\pi}m_s\left\{3\frac{M_V^2}{m_s^2}+\frac{m_s^2}{4M_V^2}\left(1-\frac{4M_V^2}{m_s^2}\right)\right\} \\
&\times\left(1-\frac{4M_V^2}{m_s^2}\right)^{1/2}\left(1-\frac{1}{2}\delta_{VZ}\right) \quad \text{(A.7)}
\end{aligned}$$

with

$$g_{sVV} = \epsilon_h g_{hVV} + \epsilon_H g_{HVV} = \epsilon_h\sin(\beta+\alpha)+\epsilon_H\cos(\beta+\alpha), \quad \text{(A.8)}$$

where $\delta_{VZ} = 1, 0$ for $V = Z, W$ and $g_W = g$ and $g_Z = g/\cos\theta_W$. ϵ_h and ϵ_H are the saxion-Higgs mixing components, which are given by

$$\begin{aligned}
\epsilon_h &= \left(\frac{1}{m_h^2-m_s^2}\right)\left(\frac{v\sin 2\beta}{2v_{PQ}}\right)\left\{m_A^2\cos(\beta-\alpha)-\frac{4\mu^2\sin(\alpha+\beta)}{\sin 2\beta}\right\}, \quad \text{(A.9)} \\
\epsilon_H &= \left(\frac{1}{m_H^2-m_s^2}\right)\left(\frac{v\sin 2\beta}{2v_{PQ}}\right)\left\{m_A^2\sin(\beta-\alpha)-\frac{4\mu^2\cos(\alpha+\beta)}{\sin 2\beta}\right\}. \quad \text{(A.10)}
\end{aligned}$$

- $s \to f\bar{f}$

$$\Gamma(s \to f\bar{f}) = \frac{N_c}{16\pi}\frac{m_f^2}{v^2} g_{sff}^2 m_s \left(1 - \frac{4m_f^2}{m_s^2}\right)^{3/2} \tag{A.11}$$

with

$$\begin{aligned} g_{sff} &= \epsilon_h g_{hff} + \epsilon_H g_{Hff} \\ &= \begin{cases} \frac{1}{\sin\beta}\left(-\epsilon_h \cos\alpha + \epsilon_H \sin\alpha\right), \text{ for up-type fermions,} \\ \frac{1}{\cos\beta}\left(-\epsilon_h \sin\alpha - \epsilon_H \cos\alpha\right), \text{ for down-type fermions.} \end{cases} \end{aligned} \tag{A.12}$$

- $s \to \widetilde{Z}_i\widetilde{Z}_j \;/\; \widetilde{W}_i\widetilde{W}_j$

$$\Gamma(s \to \widetilde{W}_i^+\widetilde{W}_i^-) = \frac{g^2}{4\pi}\left|\Sigma_i^s\right|^2 m_s \left(1 - \frac{4m_{\widetilde{W}_i}^2}{m_s^2}\right)^{3/2}, \tag{A.13}$$

$$\begin{aligned} \Gamma(s \to \widetilde{W}_1^+\widetilde{W}_2^-) &= \Gamma(s \to \widetilde{W}_1^-\widetilde{W}_2^+) \\ &= \frac{g^2}{16\pi} m_s \lambda^{1/2}\left(1, \frac{m_{\widetilde{W}_1}^2}{m_s^2}, \frac{m_{\widetilde{W}_2}^2}{m_s^2}\right) \end{aligned} \tag{A.14}$$

$$\begin{aligned} &\times \left[\left|\Sigma^s\right|^2 \left\{1 - \left(\frac{m_{\widetilde{W}_2} + m_{\widetilde{W}_1}}{m_s}\right)^2\right\}\right. \\ &\left. + \left|\Pi^s\right|^2 \left\{1 - \left(\frac{m_{\widetilde{W}_2} - m_{\widetilde{W}_1}}{m_s}\right)^2\right\}\right]. \end{aligned} \tag{A.15}$$

$$\begin{aligned} \Gamma(s \to \widetilde{Z}_i\widetilde{Z}_j) &= \frac{1}{8\pi} m_s \left(\Xi_{ij}^s + \Xi_{ji}^s\right)^2 \left[1 - \left\{\frac{m_{\widetilde{Z}_i} + (-1)^{\theta_i+\theta_j} m_{\widetilde{Z}_j}}{m_s}\right\}^2\right] \\ &\times \lambda^{1/2}\left(1, \frac{m_{\widetilde{Z}_i}^2}{m_s^2}, \frac{m_{\widetilde{Z}_j}^2}{m_s^2}\right)\left(1 - \frac{1}{2}\delta_{ij}\right), \end{aligned} \tag{A.16}$$

where θ_i is 1(0) if i-th eigenvalue of neutralino mass matrix is negative (positive) and $m_{\widetilde{Z}_i}$ is always positive. $\theta_{\widetilde{W}_i}$ is 1(0) if i-th eigenvalue of chargino mass matrix is negative (positive) and $m_{\widetilde{W}_i}$ is always positive. The neutralino couplings are given by

$$\Sigma_1^s = \epsilon_h S_1^h + \epsilon_H S_1^H - \frac{c_H \mu}{4g v_{PQ}} S_1^s, \tag{A.17}$$

$$\Sigma_2^s = \epsilon_h S_2^h + \epsilon_H S_2^H - \frac{c_H \mu}{4g v_{PQ}} S_2^s, \tag{A.18}$$

$$\Sigma^s = \epsilon_h S^h + \epsilon_H S^H - \frac{c_H \mu}{2g v_{PQ}} S^s, \tag{A.19}$$

$$\Pi^s = \epsilon_h P^h + \epsilon_H P^H - \frac{c_H \mu}{2g v_{PQ}} P^s, \tag{A.20}$$

$$\Xi_{ij}^s = \epsilon_h X_{ij}^h + \epsilon_H X_{ij}^H - \frac{c_H \mu}{2\sqrt{2} v_{PQ}} X_{ij}^s, \tag{A.21}$$

where

$$X^s_{ij} = (-1)^{\theta_i+\theta_j} v_1^{(i)} v_2^{(j)}, \tag{A.22}$$

$$S^s_1 = (-1)^{\theta_{\widetilde{W}_1}} \cos\gamma_L \cos\gamma_R, \tag{A.23}$$

$$S^s_2 = -(-1)^{\theta_{\widetilde{W}_2}} \theta_x \theta_y \sin\gamma_L \sin\gamma_R, \tag{A.24}$$

$$S^s = \frac{1}{2}\left\{(-1)^{\theta_{\widetilde{W}_1}} \theta_y \cos\gamma_L \sin\gamma_R - (-1)^{\theta_{\widetilde{W}_2}} \theta_x \sin\gamma_L \cos\gamma_R\right\}, \tag{A.25}$$

$$P^s = \frac{1}{2}\left\{(-1)^{\theta_{\widetilde{W}_1}} \theta_y \cos\gamma_L \sin\gamma_R + (-1)^{\theta_{\widetilde{W}_2}} \theta_x \sin\gamma_L \cos\gamma_R\right\}, \tag{A.26}$$

and

$$S^h_1 = \frac{1}{2}(-1)^{\theta_{\widetilde{W}_1}} \left[\sin\alpha \sin\gamma_R \cos\gamma_L + \cos\alpha \sin\gamma_L \cos\gamma_R\right], \tag{A.27}$$

$$S^h_2 = \frac{1}{2}(-1)^{\theta_{\widetilde{W}_2}+1} \theta_x \theta_y \left[\sin\alpha \cos\gamma_R \sin\gamma_L + \cos\alpha \cos\gamma_L \sin\gamma_R\right], \tag{A.28}$$

$$\begin{aligned} S^h = \frac{1}{2}\Big[&-(-1)^{\theta_{\widetilde{W}_1}} \theta_x \sin\gamma_R \sin\gamma_L \sin\alpha + (-1)^{\theta_{\widetilde{W}_1}} \theta_x \cos\gamma_R \cos\gamma_L \cos\alpha \\ &-(-1)^{\theta_{\widetilde{W}_2}} \theta_y \sin\gamma_R \sin\gamma_L \cos\alpha + (-1)^{\theta_{\widetilde{W}_2}} \theta_y \cos\gamma_R \cos\gamma_L \sin\alpha\Big], \end{aligned} \tag{A.29}$$

$$\begin{aligned} P^h = \frac{1}{2}\Big[&+(-1)^{\theta_{\widetilde{W}_1}} \theta_x \sin\gamma_R \sin\gamma_L \sin\alpha - (-1)^{\theta_{\widetilde{W}_1}} \theta_x \cos\gamma_R \cos\gamma_L \cos\alpha \\ &-(-1)^{\theta_{\widetilde{W}_2}} \theta_y \sin\gamma_R \sin\gamma_L \cos\alpha + (-1)^{\theta_{\widetilde{W}_2}} \theta_y \cos\gamma_R \cos\gamma_L \sin\alpha\Big], \end{aligned} \tag{A.30}$$

$$X^h_{ij} = -\frac{1}{2}(-1)^{\theta_i+\theta_j} \left(v_2^{(i)} \sin\alpha - v_1^{(i)} \cos\alpha\right)\left(g v_3^{(j)} - g' v_4^{(j)}\right). \tag{A.31}$$

The couplings of the heavy scalar H can be obtained from those of h by replacing $\cos\alpha \to -\sin\alpha$ and $\sin\alpha \to \cos\alpha$. $v_i^{(j)}$ is the neutralino mixing component and $\gamma_{L,R}$ is chargino mixing angle. They are defined in Ref. [38].

- $s \to \tilde{f}_i \tilde{f}_j$

$$\Gamma(s \to \tilde{f}_i \tilde{f}_j) = \frac{\left|\epsilon_h \mathcal{A}^h_{\tilde{f}_i\tilde{f}_j} + \epsilon_H \mathcal{A}^H_{\tilde{f}_i\tilde{f}_j}\right|^2}{16\pi m_s} N_c(f) \lambda^{1/2}\left(1, \frac{m^2_{\tilde{f}_i}}{m^2_s}, \frac{m^2_{\tilde{f}_j}}{m^2_s}\right), \tag{A.32}$$

where

$$\mathcal{A}^{h,H}_{\tilde{f}_1\tilde{f}_1} = \mathcal{A}^{h,H}_{\tilde{f}_L\tilde{f}_L} \cos^2\theta_f + \mathcal{A}^{h,H}_{\tilde{f}_R\tilde{f}_R} \sin^2\theta_f - 2\mathcal{A}^{h,H}_{\tilde{f}_L\tilde{f}_R} \cos\theta_f \sin\theta_f, \tag{A.33}$$

$$\mathcal{A}^{h,H}_{\tilde{f}_2\tilde{f}_2} = \mathcal{A}^{h,H}_{\tilde{f}_L\tilde{f}_L} \sin^2\theta_f + \mathcal{A}^{h,H}_{\tilde{f}_R\tilde{f}_R} \cos^2\theta_f + 2\mathcal{A}^{h,H}_{\tilde{f}_L\tilde{f}_R} \cos\theta_f \sin\theta_f, \tag{A.34}$$

$$\mathcal{A}^{h,H}_{\tilde{f}_1\tilde{f}_2} = \mathcal{A}^{h,H}_{\tilde{f}_L\tilde{f}_L} \cos\theta_f \sin\theta_f - \mathcal{A}^{h,H}_{\tilde{f}_R\tilde{f}_R} \cos\theta_f \sin\theta_f + 2\mathcal{A}^{h,H}_{\tilde{f}_L\tilde{f}_R} \cos 2\theta_f, \tag{A.35}$$

$$\mathcal{A}^{h,H}_{\tilde{f}_2\tilde{f}_1} = \mathcal{A}^{h,H}_{\tilde{f}_1\tilde{f}_2} \tag{A.36}$$

with

$$\mathcal{A}^h_{\tilde{u}_L\tilde{u}_L} = g\left[M_W\left(\frac{1}{2} - \frac{1}{6}\tan^2\theta_W\right)\sin(\beta-\alpha) - \frac{m^2_u \cos\alpha}{M_W \sin\beta}\right], \tag{A.37}$$

$$\mathcal{A}^h_{\tilde{u}_R\tilde{u}_R} = g\left[\frac{2}{3}M_W\tan^2\theta_W\sin(\beta-\alpha) - \frac{m_u^2\cos\alpha}{M_W\sin\beta}\right], \tag{A.38}$$

$$\mathcal{A}^h_{\tilde{u}_L\tilde{u}_R} = \frac{gm_u}{2M_W\sin\beta}\left(-\mu\sin\alpha + A_u\cos\alpha\right), \tag{A.39}$$

$$\mathcal{A}^H_{\tilde{u}_L\tilde{u}_L} = g\left[-M_W\left(\frac{1}{2} - \frac{1}{6}\tan^2\theta_W\right)\cos(\beta-\alpha) + \frac{m_u^2\sin\alpha}{M_W\sin\beta}\right], \tag{A.40}$$

$$\mathcal{A}^H_{\tilde{u}_R\tilde{u}_R} = g\left[-\frac{2}{3}M_W\tan^2\theta_W\cos(\beta-\alpha) + \frac{m_u^2\sin\alpha}{M_W\sin\beta}\right], \tag{A.41}$$

$$\mathcal{A}^H_{\tilde{u}_L\tilde{u}_R} = \frac{gm_u}{2M_W\sin\beta}\left(-\mu\cos\alpha - A_u\sin\alpha\right), \tag{A.42}$$

$$\mathcal{A}^h_{\tilde{d}_L\tilde{d}_L} = g\left[M_W\left(-\frac{1}{2} - \frac{1}{6}\tan^2\theta_W\right)\sin(\beta-\alpha) - \frac{m_d^2\sin\alpha}{M_W\cos\beta}\right], \tag{A.43}$$

$$\mathcal{A}^h_{\tilde{d}_R\tilde{d}_R} = g\left[-\frac{1}{3}M_W\tan^2\theta_W\sin(\beta-\alpha) - \frac{m_d^2\sin\alpha}{M_W\cos\beta}\right], \tag{A.44}$$

$$\mathcal{A}^h_{\tilde{d}_L\tilde{d}_R} = \frac{gm_d}{2M_W\cos\beta}\left(-\mu\cos\alpha + A_d\sin\alpha\right), \tag{A.45}$$

$$\mathcal{A}^H_{\tilde{d}_L\tilde{d}_L} = g\left[M_W\left(\frac{1}{2} + \frac{1}{6}\tan^2\theta_W\right)\cos(\beta-\alpha) - \frac{m_d^2\cos\alpha}{M_W\cos\beta}\right], \tag{A.46}$$

$$\mathcal{A}^H_{\tilde{d}_R\tilde{d}_R} = g\left[\frac{1}{3}M_W\tan^2\theta_W\cos(\beta-\alpha) - \frac{m_d^2\cos\alpha}{M_W\cos\beta}\right], \tag{A.47}$$

$$\mathcal{A}^H_{\tilde{d}_L\tilde{d}_R} = \frac{gm_d}{2M_W\cos\beta}\left(\mu\sin\alpha + A_d\cos\alpha\right). \tag{A.48}$$

θ_f is sfermion mixing angle, which is defined by Ref. [38].

- $\tilde{a} \to \widetilde{Z}_i\phi$

$$\Gamma(\tilde{a}\to\widetilde{Z}_i\phi) = \frac{1}{16\pi}\left(\Lambda^i_{\tilde{a}\widetilde{Z}\phi}\right)^2 m_{\tilde{a}}\lambda^{1/2}\left(1, \frac{m^2_{\widetilde{Z}_i}}{m^2_{\tilde{a}}}, \frac{m^2_\phi}{m^2_{\tilde{a}}}\right) \times\left[\left(1 + \frac{m^2_{\widetilde{Z}_i}}{m^2_{\tilde{a}}} - \frac{m^2_\phi}{m^2_{\tilde{a}}}\right) + 2(-1)^{\theta_i+\theta_{\tilde{a}}}\left(1-2\delta_{A\phi}\right)\frac{m_{\widetilde{Z}_i}}{m_{\tilde{a}}}\right], \tag{A.49}$$

for $\phi = h, H, A$. The couplings are given by

$$\Lambda^i_{\tilde{a}\tilde{Z}h} = X^h_{i0} + X^h_{0i} - \frac{c_H\mu}{\sqrt{2}v_{PQ}}T^i_{\tilde{a}\tilde{Z}h}, \tag{A.50}$$

$$\Lambda^i_{\tilde{a}\tilde{Z}H} = X^H_{i0} + X^H_{0i} - \frac{c_H\mu}{\sqrt{2}v_{PQ}}T^i_{\tilde{a}\tilde{Z}H}, \tag{A.51}$$

$$\Lambda^i_{\tilde{a}\tilde{Z}A} = X^A_{i0} + X^A_{0i} - \frac{c_H\mu}{\sqrt{2}v_{PQ}}T^i_{\tilde{a}\tilde{Z}A}, \tag{A.52}$$

where $X^{h,H}_{i0}$ is given in Eq. (A.31), X^A_{ij} is given by

$$X^A_{ij} = \frac{1}{2}(-1)^{\theta_i+\theta_j}\left(v_2^{(i)}\sin\beta - v_1^{(i)}\cos\beta\right)\left(gv_3^{(j)} - g'v_4^{(j)}\right), \tag{A.53}$$

and $T^i_{\tilde{a}\tilde{Z}\phi}$ are given by

$$T^i_{\tilde{a}\tilde{Z}h} = (-1)^{\theta_i+\theta_{\tilde{a}}}\left(v_1^{(i)}\sin\alpha + v_2^{(i)}\cos\alpha\right), \tag{A.54}$$

$$T^i_{\tilde{a}\tilde{Z}H} = (-1)^{\theta_i+\theta_{\tilde{a}}}\left(v_1^{(i)}\cos\alpha - v_2^{(i)}\sin\alpha\right), \tag{A.55}$$

$$T^i_{\tilde{a}\tilde{Z}G^0} = (-1)^{\theta_i+\theta_{\tilde{a}}+1}\left(v_1^{(i)}\cos\beta - v_2^{(i)}\sin\beta\right), \tag{A.56}$$

$$T^i_{\tilde{a}\tilde{Z}A} = (-1)^{\theta_i+\theta_{\tilde{a}}+1}\left(-v_1^{(i)}\sin\beta + v_2^{(i)}\cos\beta\right). \tag{A.57}$$

$v_0^{(i)}$ and $v_i^{(0)}$ are axino-neutalino mixing components, which are given by

$$v_0^{(0)} = 1, \tag{A.58}$$

$$v_0^{(i)} = -\frac{c_H\mu v}{v_{PQ}}\frac{v_1^{(i)}\cos\beta + v_2^{(i)}\sin\beta}{m_{\tilde{a}} - m_{\tilde{Z}_i}(-1)^{\theta_i}}, \tag{A.59}$$

$$v_i^{(0)} = \sum_{j=1}^{4}\frac{c_H\mu v}{v_{PQ}}\frac{v_i^{(j)}\left(v_1^{(j)}\cos\beta + v_2^{(j)}\sin\beta\right)}{m_{\tilde{a}} - m_{\tilde{Z}_j}(-1)^{\theta_j}}, \tag{A.60}$$

for $i = 1, \cdots, 4$.

- $\tilde{a} \to \widetilde{W}_i^{\pm}H^{\mp}$

$$\begin{aligned}\Gamma(\tilde{a} \to \widetilde{W}_i^- H^+) &= \Gamma(\tilde{a} \to \widetilde{W}_i^+ H^-) \\ &= \frac{1}{16\pi}m_{\tilde{a}}\lambda^{1/2}\left(1, \frac{m^2_{\widetilde{W}_i}}{m^2_{\tilde{a}}}, \frac{m^2_{H^+}}{m^2_{\tilde{a}}}\right) &\text{(A.61)}\\ &\quad\times\left[\left(a_i^2+b_i^2\right)\left(1 + \frac{m^2_{\widetilde{W}_i}}{m^2_{\tilde{a}}} - \frac{m^2_{H^+}}{m^2_{\tilde{a}}}\right) + 2\left(a_i^2 - b_i^2\right)\frac{m_{\widetilde{W}_i}}{m_{\tilde{a}}}\right] &\text{(A.62)}\end{aligned}$$

The couplings are given by

$$a_1 = \frac{1}{2}\left\{(-1)^{\theta_{\widetilde{W}_1}}\cos\beta\Lambda_2^{(0)} - (-1)^{\theta_{\tilde{a}}}\sin\beta\Lambda_4^{(0)}\right\}, \tag{A.63}$$

$$b_1 = \frac{1}{2}\left\{(-1)^{\theta_{\widetilde{W}_1}}\cos\beta\Lambda_2^{(0)} + (-1)^{\theta_{\tilde{a}}}\sin\beta\Lambda_4^{(0)}\right\}, \tag{A.64}$$

$$a_2 = \frac{1}{2}\left\{(-1)^{\theta_{\widetilde{W}_2}}\theta_y\cos\beta\Lambda_1^{(0)} - (-1)^{\theta_{\tilde{a}}}\theta_x\sin\beta\Lambda_3^{(0)}\right\}, \tag{A.65}$$

$$b_2 = \frac{1}{2}\left\{(-1)^{\theta_{\widetilde{W}_2}}\theta_y\cos\beta\Lambda_1^{(0)} + (-1)^{\theta_{\tilde{a}}}\theta_x\sin\beta\Lambda_3^{(0)}\right\}, \tag{A.66}$$

where

$$\Lambda_1^{(0)} = A_1^{(0)} + \frac{c_H \mu}{v_{PQ}} (-1)^{\theta_{\tilde{a}}} \tan\beta \sin\gamma_R, \tag{A.67}$$

$$\Lambda_2^{(0)} = A_2^{(0)} - \frac{c_H \mu}{v_{PQ}} (-1)^{\theta_{\tilde{a}}} \tan\beta \cos\gamma_R, \tag{A.68}$$

$$\Lambda_3^{(0)} = A_3^{(0)} - \frac{c_H \mu}{v_{PQ}} (-1)^{\theta_{\tilde{a}}} \cot\beta \sin\gamma_L, \tag{A.69}$$

$$\Lambda_4^{(0)} = A_4^{(0)} + \frac{c_H \mu}{v_{PQ}} (-1)^{\theta_{\tilde{a}}} \cot\beta \cos\gamma_L, \tag{A.70}$$

and

$$A_1^{(0)} = -\frac{1}{\sqrt{2}} \left(g v_3^{(0)} + g' v_4^{(0)} \right) \sin\gamma_R - g v_1^{(0)} \cos\gamma_R, \tag{A.71}$$

$$A_2^{(0)} = \frac{1}{\sqrt{2}} \left(g v_3^{(0)} + g' v_4^{(0)} \right) \cos\gamma_R - g v_1^{(0)} \sin\gamma_R, \tag{A.72}$$

$$A_3^{(0)} = -\frac{1}{\sqrt{2}} \left(g v_3^{(0)} + g' v_4^{(0)} \right) \sin\gamma_L + g v_2^{(0)} \cos\gamma_L, \tag{A.73}$$

$$A_4^{(0)} = \frac{1}{\sqrt{2}} \left(g v_3^{(0)} + g' v_4^{(0)} \right) \cos\gamma_L + g v_2^{(0)} \sin\gamma_L. \tag{A.74}$$

$\theta_{\tilde{a}}$ is 1(0) if axino mass term is negative (positive).

- $\tilde{a} \to \widetilde{Z}_i Z$

$$\begin{aligned} \Gamma(\tilde{a} \to \widetilde{Z}_i Z) = \frac{1}{4\pi} |W_{i0}|^2 m_{\tilde{a}} \lambda^{1/2} \left(1, \frac{m_{\widetilde{Z}_i}^2}{m_{\tilde{a}}^2}, \frac{M_Z^2}{m_{\tilde{a}}^2} \right) \\ \times \left[\left(1 + \frac{m_{\widetilde{Z}_i}^2}{m_{\tilde{a}}^2} - 2\frac{M_Z^2}{m_{\tilde{a}}^2} \right) \right. \\ \left. + \left(\frac{m_{\tilde{a}}^2}{M_Z^2} \right) \left(1 - \frac{m_{\widetilde{Z}_i}^2}{m_{\tilde{a}}^2} \right)^2 + 6(-1)^{\theta_i + \theta_{\tilde{a}}} \frac{m_{\widetilde{Z}_i}}{m_{\tilde{a}}} \right], \end{aligned} \tag{A.75}$$

where

$$W_{i0} = \frac{1}{4} \sqrt{g^2 + g'^2} (-i)^{\theta_i} (i)^{\theta_{\tilde{a}}} \left(v_1^{(i)} v_1^{(0)} - v_2^{(i)} v_2^{(0)} \right). \tag{A.76}$$

- $\tilde{a} \to \widetilde{W}_i^{\pm} W^{\mp}$

$$\begin{aligned} \Gamma(\tilde{a} \to \widetilde{W}_i^- W^+) &= \Gamma(\tilde{a} \to \widetilde{W}_i^+ W^-) \\ &= \frac{g^2}{16\pi} m_{\tilde{a}} \lambda^{1/2} \left(1, \frac{m_{\widetilde{W}_i}^2}{m_{\tilde{a}}^2}, \frac{M_W^2}{m_{\tilde{a}}^2} \right) \\ &\quad \times \left[\left(X_i^{0\,2} + Y_i^{0\,2} \right) \left\{ \left(1 + \frac{m_{\widetilde{W}_i}^2}{m_{\tilde{a}}^2} - 2\frac{M_W^2}{m_{\tilde{a}}^2} \right) \right. \right. \end{aligned}$$

$$+\left(\frac{m_{\tilde{a}}^2}{M_W^2}\right)\left(1-\frac{m_{\widetilde{W}_i}^2}{m_{\tilde{a}}^2}\right)^2\Bigg\}-6\left(X_i^{0\,2}-Y_i^{0\,2}\right)\frac{m_{\widetilde{W}_i}}{m_{\tilde{a}}}\Bigg]. \quad \text{(A.77)}$$

The couplings are given by

$$\begin{aligned}
X_1^0 &= \frac{1}{2}\Bigg[(-1)^{\theta_{\widetilde{W}_1}+\theta_{\tilde{a}}}\left(\frac{\cos\gamma_R}{\sqrt{2}}v_1^{(0)}+\sin\gamma_R v_3^{(0)}\right) \\
&\quad -\frac{\cos\gamma_L}{\sqrt{2}}v_2^{(0)}+\sin\gamma_L v_3^{(0)}\Bigg], \qquad \text{(A.78)}\\
X_2^0 &= \frac{1}{2}\Bigg[(-1)^{\theta_{\widetilde{W}_2}+\theta_{\tilde{a}}}\theta_y\left(\frac{-\sin\gamma_R}{\sqrt{2}}v_1^{(0)}+\cos\gamma_R v_3^{(0)}\right) \\
&\quad +\theta_x\left(\frac{\sin\gamma_L}{\sqrt{2}}v_2^{(0)}+\cos\gamma_L v_3^{(0)}\right)\Bigg], \qquad \text{(A.79)}\\
Y_1^0 &= \frac{1}{2}\Bigg[-(-1)^{\theta_{\widetilde{W}_1}+\theta_{\tilde{a}}}\left(\frac{\cos\gamma_R}{\sqrt{2}}v_1^{(0)}+\sin\gamma_R v_3^{(0)}\right) \\
&\quad -\frac{\cos\gamma_L}{\sqrt{2}}v_2^{(0)}+\sin\gamma_L v_3^{(0)}\Bigg], \qquad \text{(A.80)}\\
Y_2^0 &= \frac{1}{2}\Bigg[-(-1)^{\theta_{\widetilde{W}_2}+\theta_{\tilde{a}}}\theta_y\left(\frac{-\sin\gamma_R}{\sqrt{2}}v_1^{(0)}+\cos\gamma_R v_3^{(0)}\right) \\
&\quad +\theta_x\left(\frac{\sin\gamma_L}{\sqrt{2}}v_2^{(0)}+\cos\gamma_L v_3^{(0)}\right)\Bigg]. \qquad \text{(A.81)}
\end{aligned}$$

- $\tilde{a}\to f\tilde{f}_k$

$$\begin{aligned}
\Gamma(\tilde{a}\to f\tilde{f}_k) &= \frac{N_c m_{\tilde{a}}}{16\pi}\lambda^{1/2}\left(1,\frac{m_{\tilde{f}_k}^2}{m_{\tilde{a}}^2},\frac{m_f^2}{m_{\tilde{a}}^2}\right) \\
&\quad\times\Bigg[|a_f^k|^2\left\{\left(1+\frac{m_f}{m_{\tilde{a}}}\right)^2-\frac{m_{\tilde{f}_k}^2}{m_{\tilde{a}}^2}\right\} \\
&\quad +|b_f^k|^2\left\{\left(1-\frac{m_f}{m_{\tilde{a}}}\right)^2-\frac{m_{\tilde{f}_k}^2}{m_{\tilde{a}}^2}\right\}\Bigg], \qquad \text{(A.82)}
\end{aligned}$$

where

$$\begin{aligned}
a_u^1 &= \frac{1}{2}\left[\left\{iA_{\tilde{a}}^u-(i)^{\theta_{\tilde{a}}}f_u v_1^{(0)}\right\}\cos\theta_u-\left\{iB_{\tilde{a}}^u-(-i)^{\theta_{\tilde{a}}}f_u v_1^{(0)}\right\}\sin\theta_u\right], \qquad \text{(A.83)}\\
b_u^1 &= \frac{1}{2}\left[\left\{-iA_{\tilde{a}}^u-(i)^{\theta_{\tilde{a}}}f_u v_1^{(0)}\right\}\cos\theta_u-\left\{iB_{\tilde{a}}^u+(-i)^{\theta_{\tilde{a}}}f_u v_1^{(0)}\right\}\sin\theta_u\right], \qquad \text{(A.84)}\\
a_d^1 &= \frac{1}{2}\left[\left\{iA_{\tilde{a}}^d-(i)^{\theta_{\tilde{a}}}f_d v_2^{(0)}\right\}\cos\theta_d-\left\{iB_{\tilde{a}}^d-(-i)^{\theta_{\tilde{a}}}f_d v_2^{(0)}\right\}\sin\theta_d\right], \qquad \text{(A.85)}\\
b_d^1 &= \frac{1}{2}\left[\left\{-iA_{\tilde{a}}^d-(i)^{\theta_{\tilde{a}}}f_d v_2^{(0)}\right\}\cos\theta_d-\left\{iB_{\tilde{a}}^d+(-i)^{\theta_{\tilde{a}}}f_d v_2^{(0)}\right\}\sin\theta_d\right], \qquad \text{(A.86)}
\end{aligned}$$

$$a_u^2 = \frac{1}{2}\left[\left\{iA_{\tilde{a}}^u-(i)^{\theta_{\tilde{a}}}f_u v_1^{(0)}\right\}\sin\theta_u+\left\{iB_{\tilde{a}}^u-(-i)^{\theta_{\tilde{a}}}f_u v_1^{(0)}\right\}\cos\theta_u\right], \qquad \text{(A.87)}$$

$$b_u^2 = \frac{1}{2}\left[\left\{-iA_{\tilde{a}}^u - (i)^{\theta_{\tilde{a}}} f_u v_1^{(0)}\right\}\sin\theta_u + \left\{iB_{\tilde{a}}^u + (-i)^{\theta_{\tilde{a}}} f_u v_1^{(0)}\right\}\cos\theta_u\right], \quad \text{(A.88)}$$

$$a_d^2 = \frac{1}{2}\left[\left\{iA_{\tilde{a}}^d - (i)^{\theta_{\tilde{a}}} f_d v_2^{(0)}\right\}\sin\theta_d + \left\{iB_{\tilde{a}}^d - (-i)^{\theta_{\tilde{a}}} f_d v_2^{(0)}\right\}\cos\theta_d\right], \quad \text{(A.89)}$$

$$b_d^2 = \frac{1}{2}\left[\left\{-iA_{\tilde{a}}^d - (i)^{\theta_{\tilde{a}}} f_d v_2^{(0)}\right\}\sin\theta_d + \left\{iB_{\tilde{a}}^d + (-i)^{\theta_{\tilde{a}}} f_d v_2^{(0)}\right\}\cos\theta_d\right], \quad \text{(A.90)}$$

with

$$A_{\tilde{a}}^u = \frac{(-i)^{\theta_{\tilde{a}}-1}}{\sqrt{2}}\left[g v_3^{(0)} + \frac{g'}{3} v_4^{(0)}\right], \quad \text{(A.91)}$$

$$A_{\tilde{a}}^d = \frac{(-i)^{\theta_{\tilde{a}}-1}}{\sqrt{2}}\left[-g v_3^{(0)} + \frac{g'}{3} v_4^{(0)}\right], \quad \text{(A.92)}$$

$$B_{\tilde{a}}^u = \frac{4}{3\sqrt{2}} g'(i)^{\theta_{\tilde{a}}-1} v_4^{(0)}, \quad \text{(A.93)}$$

$$B_{\tilde{a}}^d = -\frac{2}{3\sqrt{2}} g'(i)^{\theta_{\tilde{a}}-1} v_4^{(0)}. \quad \text{(A.94)}$$

Here $f_{u,d}$ is the Yukawa coupling constant.

References

[1] R. D. Peccei and H. R. Quinn, Phys. Rev. Lett. **38**, 1440 (1977).

[2] S. Weinberg, *Phys. Rev. Lett.* **40** (223) 1978; F. Wilczek, *Phys. Rev. Lett.* **40** (279) 1978.

[3] J. E. Kim, Phys. Rev. Lett. **43** (1979) 103; M. A. Shifman, A. Vainstein and V. I. Zakharov, Nucl. Phys. **B166**(1980) 493.

[4] M. Dine, W. Fischler and M. Srednicki, Phys. Lett. **B104** (1981) 199; A. P. Zhitnitskii, Sov. J. Phys. **31** (1980) 260.

[5] H. P. Nilles, Phys. Rept. **110**, 1 (1984).

[6] T. Goto and M. Yamaguchi, Phys. Lett. B **276**, 103 (1992).

[7] E. J. Chun, J. E. Kim and H. P. Nilles, Phys. Lett. B **287**, 123 (1992)

[8] E. J. Chun and A. Lukas Phys. Lett. B **357**, 43 (1995).

[9] L. F. Abbott and P. Sikivie, *Phys. Lett.* **B 120** (1983) 133; J. Preskill, M. Wise and F. Wilczek, *Phys. Lett.* **B 120** (1983) 127; M. Dine and W. Fischler, *Phys. Lett.* **B 120** (1983) 137; M. Turner, *Phys. Rev.* **D 33** (1986) 889.

[10] L. Visinelli and P. Gondolo, *Phys. Rev.* **D 80** (2009) 035024.

[11] G. Jungman, M. Kamionkowski and K. Griest, Phys. Rept. **267** (1996) 195 [hep-ph/9506380].

[12] E. J. Chun, H. B. Kim and D. H. Lyth, Phys. Rev. D **62**, 125001 (2000) [hep-ph/0008139]; L. Covi, H. B. Kim, J. E. Kim and L. Roszkowski, JHEP**0105** (2001) 033; A. Brandenburg and F. D. Steffen, JCAP **0408** (2004) 008; A. Strumia, JHEP **1006** (2010) 036; K. -Y. Choi, L. Covi, J. E. Kim and L. Roszkowski, JHEP **1204** (2012) 106; P. Graf and F. D. Steffen, JCAP **1302** (2013) 018.

[13] K. -Y. Choi, J. E. Kim, H. M. Lee and O. Seto, Phys. Rev. D **77** (2008) 123501;

[14] H. Baer, A. Lessa, S. Rajagopalan and W. Sreethawong, JCAP **1106** (2011) 031 .

[15] H. Baer, A. Lessa and W. Sreethawong, JCAP **1201** (2012) 036 .

[16] K. J. Bae, H. Baer and A. Lessa, JCAP **1304** (2013) 041.

[17] P. Graf and F. D. Steffen, JCAP **1302** (2013) 018 [arXiv:1208.2951 [hep-ph]].

[18] P. Graf and F. D. Steffen, arXiv:1302.2143 [hep-ph].

[19] J. P. Conlon and M. C. D. Marsh, arXiv:1304.1804 [hep-ph].

[20] J. Hasenkamp and J. Kersten, *Phys. Rev.* **D 82** (2010) 115029.

[21] J. E. Kim and H. P. Nilles, Phys. Lett. B **138**, 150 (1984); E. J. Chun, J. E. Kim and H. P. Nilles, Nucl. Phys. B **370**, 105 (1992).

[22] E. J. Chun, Phys. Rev. D **84** (2011) 043509

[23] K. J. Bae, K. Choi and S. H. Im, JHEP **1108**, 065 (2011) [arXiv:1106.2452 [hep-ph]].

[24] K. J. Bae, E. J. Chun and S. H. Im, JCAP **1203** (2012) 013.

[25] H. Baer, V. Barger, P. Huang, A. Mustafayev and X. Tata, Phys. Rev. Lett. **109**, 161802 (2012); H. Baer, V. Barger, P. Huang, D. Mickelson, A. Mustafayev and X. Tata, arXiv:1212.2655 (2012); H. Baer, V. Barger and D. Mickelson, arXiv:1309.2984 [hep-ph].

[26] K. J. Bae, H. Baer and E. J. Chun, arXiv:1309.0519 [hep-ph].

[27] H. Baer and A. Lessa, JHEP **1106** (2011) 027.

[28] F. Paige, S. Protopopescu, H. Baer and X. Tata, `hep-ph/0312045`; http://www.nhn.ou.edu/∼isajet/

[29] H. Baer, C. Balazs and A.Belyaev, *J. High Energy Phys.* **0203** (2002) 042.

[30] WMAP Collaboration, G. Hinshaw et al., arXiv:1212.5226 [astro-ph.CO].

[31] H. Baer, V. Barger, P. Huang, D. Mickelson, A. Mustafayev and X. Tata, Phys. Rev. D **87** (2013) 3, 035017 [arXiv:1210.3019 [hep-ph]].

[32] P. A. R. Ade *et al.* [Planck Collaboration], arXiv:1303.5076 [astro-ph.CO].

[33] E. Aprile *et al.* [XENON100 Collaboration], Phys. Rev. Lett. **109** (2012) 181301 .

[34] K. Choi, E. J. Chun and J. E. Kim, Phys. Lett. B **403** (1997) 209.

[35] K. S. Jeong and F. Takahashi, JHEP **1208**, 017 (2012)

[36] H. Baer, V. Barger and D. Mickelson, arXiv:1303.3816 [hep-ph] (Phys. Lett. **B**, in press).

[37] L. Duffy, *et. al.*, *Phys. Rev. Lett.* **95** (2005) 091304 and *Phys. Rev.* **D 74** (2006) 012006; for a review, see S. J. Asztalos, L. Rosenberg, K. van Bibber, P. Sikivie and K. Zioutas, *Ann. Rev. Nucl. Part. Sci.* **56** (2006) 293.

[38] H. Baer and X. Tata, *Weak Scale Supersymmetry: From Superfields to Scattering Events*, (Cambridge University Press, 2006).